CHARACTERIZATION OF SOL-GEL DERIVED MATERIAL MICROARRAYS

SURFACE CHARACTERIZATION AND COMPARISON OF

CONTACT VS. NON-CONTACT PRINTED

SOL-GEL DERIVED MATERIAL MICROARRAYS

By

Blake-Joseph Helka, B.Sc. (Honours)

A Thesis

Submitted to the School of Graduate Studies

In Partial Fulfillment of the Requirements

For the Degree

Master of Science

McMaster University

MASTER OF SCIENCE (2013) McMaster University

(Chemistry and Chemical Biology) Hamilton, Ontario

TITLE: Surface Characterization of Sol-Gel Derived Material Microarrays

AUTHOR: Blake-Joseph Helka, B.Sc. (Honours) (Laurentian University)

SUPERVISOR: Dr. John D. Brennan

NUBMER OF PAGES: viii, 65

Abstract

Fabrication of microarrays using sol-gel immobilization has been utilized as an approach to develop high density biosensors. Microarray fabrication using various printing techniques including pin-printing and piezoelectric ink jet printing methods has been demonstrated. However, only limited characterization to understand the encapsulated biomolecule-material interface has been reported. Herein, Chemical characterization using X-ray photoelectron spectroscopy (XPS) and infrared spectroscopy (IR) on pin-printed microarrays of sol-gel derived acetylcholinesterase (AChE) microarrays is reported. Furthermore, the *in situ* fabrication of microarrays following the sol-gel process using piezoelectric ink jet printing methods was explored. Through techniques measuring solution viscosity, surface tension and particle size, important aspects of bio-ink formulation for piezoelectric ink jet printing were identified. Combined, a greater understanding towards the fabrication and characterization of sol-gel derived microarrays was achieved through this exploratory research.

Acknowledgements

Through completion of this thesis I would like to thank my supervisor, Dr. John Brennan as well as past and present members of the Brennan research group. Over the past few years Dr. Brennan's enthusiasm and contribution for science provided me with insight towards all aspects related to research. To the members of the group, countless hours of conversation, research and non-research related helped keep me of sound mind. Further thanks to my committee for offering me guidance and support throughout me evolving research project.

I would also like to extend my thanks to the many faculty and staff of McMaster Univeristy, especially those working within the Biointerfaces Institute for all of their assistance, advice and guidance.

To my family, their constant support and belief provided me with motivation and drive. While at times it was tiring, their positive belief in me gave me inspiration. I know without them this wouldn't have been possible.

Lastly, I would like to thank my favourite little scientist, Nicole De Long for sharing in this experience and helping me close this chapter of me life.

Table of Contents

List of Figures and Tables

List of Abbreviations

AChE – acetylcholinesterase

APTES - 3-aminopropyl-trimethoxysilane

ATCh – acetythiocholine iodide

DGS – diglycerylsilane

GLS - N-(3-triethoxysilpropyl)gluconamide

HTS – high-throughput screening

IR – infrared spectroscopy

MTMS – trimethoxymethylsilane

PEG – poly(ethylene glycol)

PEI – poly(ethyleneimine)

PDC – piezoelectric dispensing capillary

PVA – poly(vinyl alcohol)

SS – sodium silicate

Si-COOH - carboxyethylsilanetriol

TEOS - tetraethylorthosilicate

TMOS - tetramethylorthosilicate

XPS – X-ray photoelectron spectroscopy

Chapter - One | Introduction

Portions of this introduction were taken from, Dahoumane, S-A. Helka, B-J. Artus, M. Aubie, B. Brennan, J.D. High Throughput Screening for the Production of Biomaterials: A New Tool for the Study of the Interactions Between Materials and Biological Species. *Handbook of Nanomaterial Properties.* Springer Scientific. Accepted May 13, 2013. [1]

1.1. High-throughput Screening and Microarray Technology

Merrifield originally proposed the concept behind combinatorial chemistry half a century ago as a method for solid-phase peptide synthesis. [2] Building on the initial one-by-one synthesis approach, work published by Furka, [3] Houghten, [4] and Lam, [5] highlighted the concepts of combinatorial chemistry decades later with methods for multicomponent peptide synthesis. The application of combinatorial chemistry within the pharmaceutical industry shifted the "bottleneck" of discovery to the screening methods utilized to assess the biological activity of various small molecules. [6,7] Today, researchers have developed numerous tools for a rapid and efficient screen and assessment of a wide range of products that collectively can be categorized under the general term of high-throughput screening (HTS). Advantages of HTS include automation, increased sample density and reduced reagent volume; minimizing the overall time and cost associated to the assessment of a single small molecule.

Microarrays stand out within the literature as an optimal platform for both high-throughput synthesis and characterization. With their development in the

mid 1990's as a method to assess gene expression, microarrays have since been used in the development of high-throughput assays to identify biomolecule interactions with other biomolecules, [8] small molecules and the identification of materials with unique properties. [9-12] Collectively, the different methods available for printing microarrays are capable of producing highly reproducible, spatially oriented patterns upon various substrates including but not limited to standard glass microscope slides, the bottom of a well within a microtiter plate and other surfaces such as silicon wafers. [13-15] A further advantage using microarrays as a platform for developing biosensors is the added ability to include all necessary components to screen samples and controls together in a highly paralleled fashion. [13]

1.2. Methods in Microarray Fabrication

Generally defined as a method for the production of highly ordered and dense patterns, microarrays are commonly produced using several methods including but not limited to, photo-, soft- or nano-lithography and contact or non-contact printing. [16] Each method is capable of producing arrays consisting of thousands to tens of thousands of "spots" per standard microscope slide (25 mm × 75 mm). Drawbacks of lithography and stamp based methods is the limited ability to produce an array element on a single substrate (lithography) or material (stamps). Despite the ability to produce high-density microwells/arrays, these techniques do not allow hundreds if not thousands of materials to be screened at once. [16] These methods are in the authors opinion more suitable for the HT

production of array based biosensors which typically include repeats of the same bio-recognition element spatially oriented onto a surface. Thus, for this thesis, only microarray formation through contact (pin-printing) and non-contact (ink jet) printing will be discussed as these methods relate to the most common methods utilized within the literature for the production and evaluation of biomaterial microarrays (Figure 1.1). Independent of printing method, the aim of each technique is the efficient production of homogeneous, (uniform spot size) high-density arrays with high precision and accuracy. Further shared among several printing modalities is control and movement of the "print head" through a power driven XYZ stage.

As the name implies, contact pin-printing refers to microarrays formed through the direct contact between a "printing" pin and the substrate (Figure 1.2A) Typically, pins are either solid or quilled (containing a slit which acts as a reservoir, Figure 1.1). With respect to solid pins, the deposited spot size and shape will be directly linked to the shape and size of the pin. For quilled pins, slit width will influence the size of the spot, while the shape of the slit reservoir will influence the volume deposited for each spot. [16] Pins are typically metallic and will allow for deposition of spots ranging from one hundred to a few hundred microns in diameter. Recently, silicon-based pins have been developed which allow for greater dimensional control and smaller deposited spot volumes. [17]

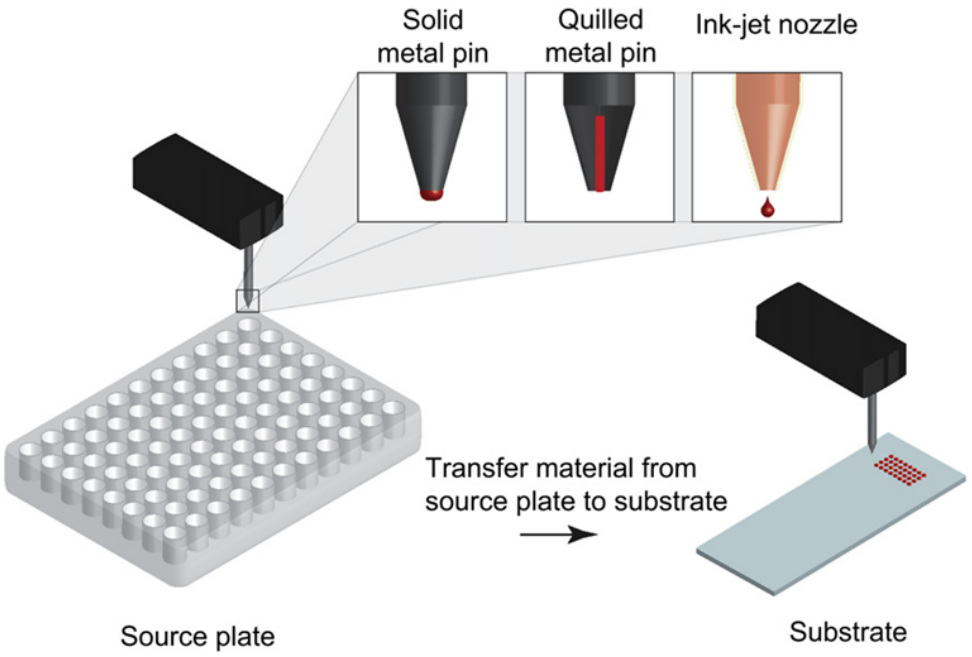

Figure 1.1: Schematic representation of different print heads used for microarray formation. Spotting solution (shown as a red solution) is typically collected from a source plate and subsequently deposited onto a substrate (commonly a microscope slide) by means of a printing pin (solid of quilled) or through an ink jet nozzle. As seen elsewhere and reprinted with permission. [9]

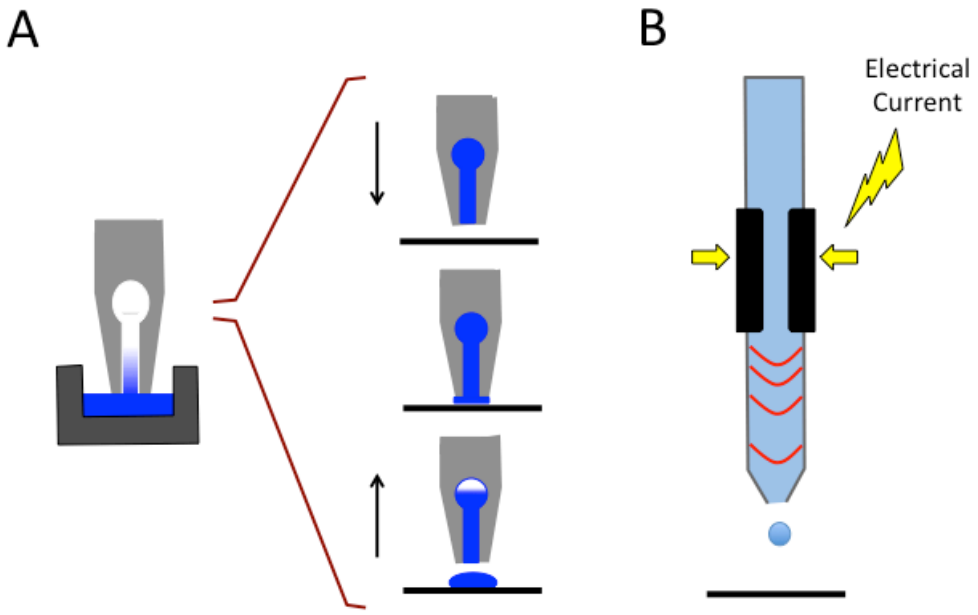

Figure 1.2: Schematic representation of microarray formation using contact pin-printing (A) and piezoelectric ink jet (B) printing methods for material deposition onto a planar surface. Images adapted from Arrayit.com, [18,] and Derby [190]

Unfortunately, the robustness of silicon-based pins often results in inconsistent spotting from pin-induced fractures in substrate coating, [16] however, recent advances using quartz based pins for increased spot density have been reported. [20] Other important parameters related to producing quality contact arrays remain independent of the pin itself. Environmental factors (temperature and humidity), and instrumental (print head travel speed and contact time) and solution (viscosity and surface tension) properties determine the "printability" of any given solution. The combination of environmental, instrumental and solution based factors which determine printability of materials make contact printing methods highly versatile and well suited for printing a range of chemically stable solutions. Many research groups have been utilizing contact printing as a method to prepare microarrays of polymers such as acrylates, acrylamides and urethanes, which generally require UV irradiation or addition of an initiator after printing to form and fix the polymer materials to the substrate surface. [20-23] For less stable polymers, an alternative approach can be utilized wherein a pre-screening and selection approach is used to first identify materials that are printable (*ie.* do not polymerize in the pin), followed by production of a more limited microarray of materials using a contact printer. [13-15]

In contrast to contact printing methods, non-contact (ink jet) printing relates to a much larger and more diverse class of printing techniques. The two main types of non-contact printing methods involved in microarray production utilize thermal and piezoelectric dispensing and can be either continuous or drop

on demand methods, where continuous refers to a steady stream of expelled droplets. Both thermal and piezoelectric printing methods form drops through the propagation of pressure within the fluid-containing chamber. Difference relate to the means used to produce drops through the creation of “pressure pulses”. In thermal printing, solution in direct contact with a heater, which raises the solution above the boiling point (up to 300 °C), forms and deforms bubbles in solution generating the required pressure pulse. In contrast, piezoelectric printing produces pressure pulses through direct mechanical action using a piezoelectric material (commonly a crystal or ceramic) as an actuator (Figure 1.2B). [16,19,24] As piezoelectric printing methods are more tunable than thermal printing methods, material research and thus microarrays are most often produced using piezoelectric printing robots, including both polymer and sol-gel derived microarrays. [25,26] The size of the expelled drops ranges from low- to mid-hundred picoliter volumes, which determin the size of the on-array spot. Alteration of drop volume, and thus spot size, can be accomplished by altering the size of the nozzle orifice, or by altering the pressure pulse through precise control of pulse duration and voltage. [27] Aside from nozzle constraints (size and applied pulse duration and/or voltage), spotting solution properties are important factors that determine the printability of a material. For example, solutions that are too viscous (typically greater than 20 mPa*s) will inhibit printing. [19,27,28] Failed printing due to materials clogging the nozzle orifice is also characteristic of ink jet printing. [16] Temperature and humidity also have significant effects (as compared

to contact printing methods) on the printability of materials and final spot shape and size, [28,29] due to evapouration of small drop sizes. [30] However, the advantage of small drop sizes is the ability to perform "drop-on-drop" printing. In this technique, multiple nozzles are used in parallel to initially spot and subsequently re-spot solutions over each other. [31] Taking advantage of this method, it may be possible to print materials that are reactive in nature (such as sol-gel derived materials), which would normally be considered unprintable owing to rapid polymerization upon mixing (akin to separately printing components A and B or an epoxy rather than mixing these prior to printing, as is required for contact printing).

1.3. Methods in Biomolecule Immobilization

Fabrication of biomolecule microarrays is typically done following traditional methods of bio-immobilization utilizing solid supports. Those include immobilization through physical adsorption, [32,33] covalent[32-34] and affinity based attachment, [35] and entrapment within a polymeric/cross-linked material [36-38] (Figure 1.3).

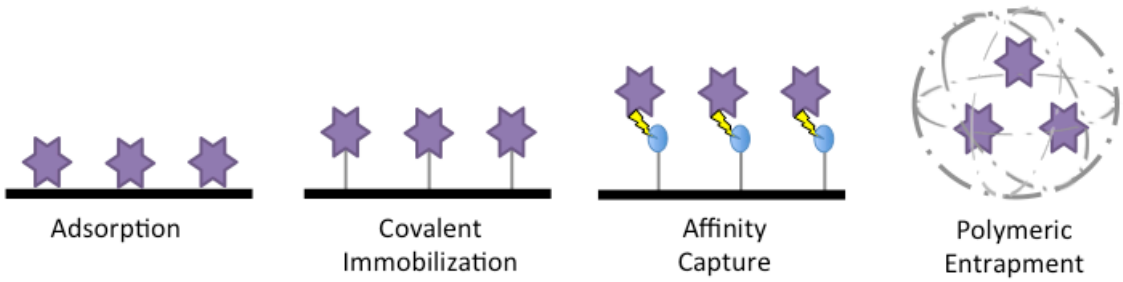

Figure 1.3: Graphical representation comparing different methods in bio-immobilization by means of adsorption, covalent and affinity based binding and entrapment within a polymeric material. Image adapted from Rupcich *et al.* [39]

In the case of this thesis, only polymeric entrapment in organic sol-gel based materials was considered. At first, interest in bio-encapsulation based research focused- around the immobilization of biomolecules within gels formed by organic polymers such as alginate and chitosan. [40] While this reason was obvious in terms of biocompatibility, the encapsulation of biomolecules within "bio-polymers" suffered limitations of an often-reversible cross-linked material and poor control over porosity. The use of inorganic precursors for encapsulation of biomolecules by the sol-gel process offered an alternative material for encapsulation with the added benefit of greater control over porosity. [41-43] Furthermore, the resulting gels are both chemically and mechanically stable offering an immobilization method resistant to biodegradation. [44]

1.4. The Sol-Gel Process for Bioimmobilization

The first example of biomolecule immobilization within an organic matrix dates back to the mid 1950's. [45] Decades later, the entrapment of various

biomolecules including enzymes, antibodies, membrane proteins, nucleic acid and whole cells within inorganic matrices were reported and still remains a prominent area of research for biosensing applications. [41,42] Silica based matrices represent the most commonly utilized materials due to their biocompatibility. Moreover, silica gels have the advantage of being transparent, which makes them promising materials for optical detection. [43] Most importantly, the synthesis of silica matrices can be performed under mild conditions of "soft chemistry" via the sol-gel process (Figure 1.4).

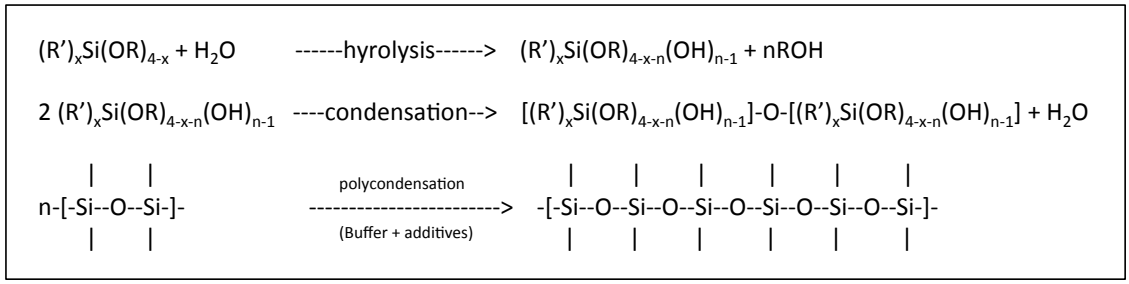

Figure 1.4: Generic scheme of the sol-gel process using traditional alkoxysilanes. The entrapment of biomolecules is performed following a general 2 step procedure where a silica precursor undergoes hydrolysis and condensation procuring a sol that undergoes gelation with the addition of a buffered aqueous component containing the biomolecule of interest. Adapted from Brennan, 2007. [42]

The sol-gel process is a synthetic route by which hydrolysis-condensation reactions generate oxide networks through polymerization of molecular precursors that can generally be defined as a two-step process. [46] The first step involves the formation of a sol. Typically, sols are produced by an acid or based catalyzed hydrolysis of an alkoxide precursors, tetramethoxysilane (TMOS) or tetraethoxysilane (TEOS) resulting in the formation of hydroxyl groups. The

subsequent condensation reaction leads to the formation of siloxane bonds (Si-O-Si) that are the origin of the silica network and result in the release of water and/or alcohol. The kinetics of the hydrolysis reaction affects the nature of hydroxylated species involved in the condensation reaction and, hence, affects the final gel structure. [46] Acidic conditions leads to microporous (pore diameters < 2 nm) networks whereas basic conditions favours mesoporous (pore diameter between 2 and 50 nm) networks. [46] The second step involves mixing the prepared sol with an often-buffered aqueous component containing the biomolecule(s) of interest in addition to additives, which can impart variations within the gel matrix, or assist in biomolecule stability. As the sol obtained evolves over time, the viscosity increases to form a hydrated gel within seconds to days, influenced by the pH and ionic strength that change the speed of the condensation reaction.

Initial work using alkoxy silanes such as TMOS and TEOS required the addition of co-solvent during the initial hydrolysis reaction. In addition to the added alcohol released during hydrolysis, the extremely acidic of basic reaction conditions were not favourable for bio-encapsulation. Work within the group led by David Avnir showed the alcohol released during hydrolysis was sufficient to homogenize the reagents with the use of sonication. [47] Based on this result, Ellerby *et al.* successfully encapsulated three metaloproteins within a TMOS based gel at biocompatible pH (> pH 5). [48] This was achieved by the addition of buffer to the sol suspension after acid catalyst and prior to enzyme addition. [48]

While success was shown in enzyme encapsulation, alcohol was still present during gelation. Several methods were developed to eliminate the presence of pre-hydrolyzed alcohol before gelation by bubbling nitrogen or air through the alcohol sol, or by alcohol evaporation from the sol before the addition of biological species. [49,50]

Another approach to the development of biofriendly sol-gel derived materials was synthesis of the silica matrix by an aqueous route using sodium silicate. While this method implies the presence of sodium ions, Brinker's group demonstrated the use of a cationic exchange resin to remove and replace sodium ions with protons. [51] This method produced an acidic sol, which through the addition of an aqueous buffered protein solution promoted condensation. In parallel, a glycerated precursor, poly(glycerol silicate), (PGS) was synthesized by adding glycerol to TMOS via catalysis with hydrochloric acid and poly(antimony(III) ethylene glycoxide) through work by Gill and Ballesteros. [52] Expanding on the notion of using glycerated silanes which release glycerol, a protein stabilizing compound during hydrolysis, Brook *et al.* developed another biocompatible sol-gel precursor diglycerlsilane (DGS) in addition to other sugar modified silanes. [53-55] Similar to the synthesis of PGS, DGS was achieved through adding glycerol to TMOS but required no catalyst for the added benefit of minimizing contaminants.

The versatility of the sol-gel process for bio-encapsulation can also be attributed to control over the silica network (pore size and distribution) that can be

optimized to different biomolecules, required assay conditions or both. Often, gel variation is altered through changes in pH, ionic strength and material additives added to the sol. Examples of gel control include the use of polymers such as poly(ethylene glycol) (PEG), and poly(vinyl alcohol) (PVA), which act as poragens creating a bimodal pore distribution within the silica matrix. [56] Furthemore, various starting silica precursors and organosilanes such as methyltrimethoxy silane (MTMS) or (3-aminopropyl)triethoxysilane (APTES) allow gel properties such as polarity to be tuned. [57] Resulting materials can be created with varying hydrophobic environments favourable for certain biomolecules. Most importantly, the sol-gel process serves as a support that contains microenvironments within pores, which in the presence of extreme conditions resists denaturation of the entrapped biomolecule. [41] In fact, immobilized bio-entities such as enzymes, [58-60] membrane bound receptors, [61,62] cells [63] and nucleic acids [64,65] within sol-gel derived materials have demonstrated the increase in their bio-stability after entrapment.

1.5. Sol-gel Derived Microarray Technology

Immobilization of biological entities within sol-gel derived materials has been extensively studied for various reasons mentioned above. Of the various biosensor formats, (monolithic affinity blocks and columns, thin films and microarrays), the most exciting and possibly least investigated applications of sol-gel derived materials remains microarrays. With few groups researching sol-gel derived microarrays, work within the groups led by Clark and Bright demonstrated

the earliest work with the field of sol-gel based biosensors. [66-69] At the turn of the century, Chan et al. [69] and Kim *et al.* [68] utilized micro pattering techniques for array production. Shortly after, Cho *et al.* [66] fabricated the first pin-printed sol-gel based microarray. While this early work highlighted the capabilities of sol-gel derived microarrays it was limited to only a handful of materials.

Given the versatility and ability to adapt materials for various biomolecules, sol-gel derived microarrays are ideally suited for investigation by HTS methods. Expanding on technology with the Bright group, Cho *et al.* [70] employed a HTS approach that evaluated the biodegradable properties of more than 600 material formulations for multiple outcomes. The first screen identified materials with the ability to release keratinocyte growth factor (KGF), a protein associated with wound healing. The second desired outcome identified materials that retained anti-fluorescein antibody activity in TEOS based gels for the purpose of developing future biosensors. Despite success, work within the Bright group shifted away from protein doped sol-gel materials and focused on developing oxygen sensing microarrays using entrapped lumiphores. [71-75]

Work within the Brennan group expanded sol-gel derived microarray technology comparing the effects of various precursors, DGS, SS and monosorbitol silane (MSS) beyond TEOS for the entrapment and fabrication of antibody-based microarrays. Additionally, effects of surface chemistry and array performance were evaluated and compared to traditional covalently immobilized antibody arrays. Along with Doong et al., the Brennan group also reported on the

design of enzymatic pin-printed arrays in a 96-well microplate format with success in evaluating on array enzymatic activity, [76] screening for Alzheimer's biomarkers [77] and small molecule kinase inhibitors. [59]

Since the takeoff of sol-gel based microarray technology, more extensive material based screening studies have been carried out. Work by Kim *et al.* involved the screening of 100,000 sol-gel based materials. [25] Materials combined several silicate monomers and intermediates, six additives and multiple buffer conditions and arrays were printed using piezo-inkjet printing methods. Of the almost 700 identified material combinations amenable to printing only a small subset of ~7 were found to be optimal at retaining the activity of the entrapped peptide, BSA and secondary rabbit based antibodies. The identified materials were also amenable to fabrication of heated sol-gel derived microarrays for the selection and subsequent entrapment of a aptamer for detection hepatitis C virus (HCV) within biological samples. [14,78,79] More recently, building on the optimized material formations, Ahn *et al.* demonstrated the ability to entrap bisphenol A (BPA), a small molecule within a gel without limiting much larger affinity based ligands. [80] Similar work printing sol-gel derived materials was carried out within the Brennan group building off their initial low-throughput screening approach that involved a systematic material screen(Figure 1.5).

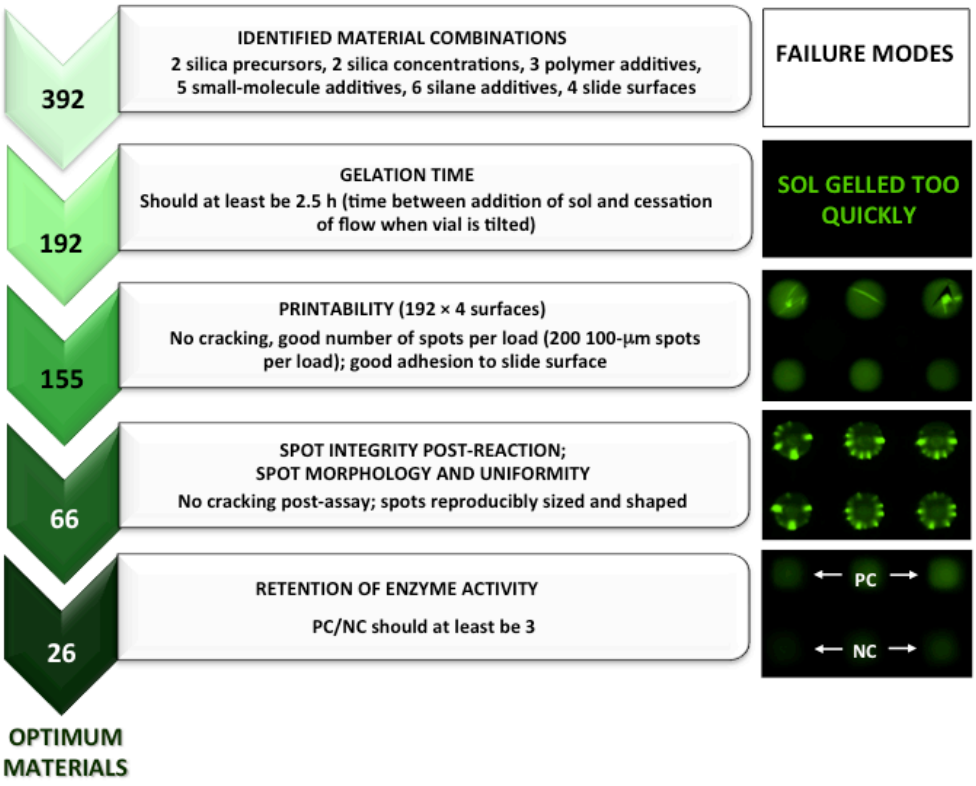

Figure 1.5: Progressional schematic of a directed material screen approach with various failure modes for the identification of optimal material formulations used in the fabrication of pin-printed sol-gel derived acetylcholinesterase (AChE) microarrays. As seen and reprinted with permission from Monton *et al.* [15]

This method implemented a series of pre-screening steps to identify sols with sufficient gelation times to avoid material gelation within the printing pin. [58] Sols were then assessed for their printability and screened by material adhesion to the substrate, uniformity, integrity and assay compatibility (ability to withstand over-printing). Materials that passed were assessed for enzymatic activity and ultimately, 26 of ~ 20,000 possible material combinations that retained a positive control (PC) to negative control (NC) ratio of greater than 3 were identified. [15] While following the similar method, Xin *et al.* encapsulated 4 kinases simultaneous and identified 2 of the original 192 printable material formulations

retained optimal activity with a multiplexed kinase assay. [13] In both cases, the targeted assay was validated on-array and their use for small molecule screening was shown through the produced on-array inhibition curves. [13,15]

1.6. HTS Methods in Microarray Characterization

Advances in microarray technology and robots have permitted HTS methodologies as powerful and rapid tools for the production of hundreds if not hundreds of thousands of new materials or microarray based sensors per day. However, this has presented a significant challenge to rapidly evaluate and characterize the varying performance/properties of the ever-increasing number of biomaterials. While the ability to completely characterize the mass-produced materials may not be possible in a timely fashion, the ability to extract relevant information from a material library can be accomplished. Parallel imaging techniques based on optical, confocal or fluorescence microscopy offer a high-throughput, low information content method for microarray characterization. With materials such as sol-gel derived materials, using simply optical microscopy, printed materials can be assessed for “failures” by identifying material combinations that result in poor spot adhesion and spot reproducibility (missing spots, improper phase separation, cracking) (Figure 1.5). [13,15] With respect to biomaterial microarrays, the use of fluorescent substrates allows assay optimization, material evaluation and in some cases the ability to perform on-array small molecule screens for the identification of ligand binding targets. [13,15] This information content can quickly identify lead materials and substantially

reduce the number of materials to be characterized by slower, often more costly methods which provide higher information content.

More advance characterization techniques including methods in spectroscopy (x-ray photoelectron spectroscopy (XPS), fourier transform infrared spectroscopy (FTIR), ect.) and mass spectrometry (matrix-assisted laser desorption/ionization mass spectrometry (MALDI-MS), time-of-flight secondary ion mass spectrometry (ToF-SIMS)) or physiochemical methods (contact angle) offer increased detail on chemical or mechanical properties of the material. In terms of chemical information, characterization methods such as XPS and Tof-SIMS are limited to providing surface properties of the materials. These methods also require operation under high vacuum and thus they do not provide information based on the hydrated, biochemically stable state of the material. With respect to XPS, quantitative chemical elemental analysis present in the top 10 nm of the sample can provide varying functional groups present such as alkyl, alcohol, amine or carbonyl based moieties. [81,82] Furthermore, it is possible to perform depth-profiling with XPS to provide a “layer-by-layer” chemical analysis of a material. [82]

For more information on chemical properties of the bulk material, FTIR gives the nature of chemical groups as well as relative amounts of different functional groups within the material. The main advantage of FTIR remains the ability to perform characterization without vacuum, thus, providing real-time data on the nature and interactions of biomaterials.

Collectively, when operating methods such as FTIR, XPS, ToF-SIMS and MALDI-MS in imaging mode in order to produce highly spatial often three-dimensional surface maps, sample preparation and the need to slowly raster and collect data over the sample can require up to several days to read a full array. As an example, Davies and coworkers analyzed the surface chemistry of 576 polymers by XPS, Tof-SIMS and water contact. [30] While this combined techniques provided a wealth of information it required just under a week to collect the data. Despite the wealth of information collected, each technique on its own with the exception of Tof-SIMS did not provide material correlations. However, correlation of multiple measurements against a specific outcome and the use of principal component analysis can help predict a basic model for controlled material properties. Perhaps one of the latest and complete examples includes the work by Hook *et al.*. [83] Using material identified from previous work, [21-23,84,85] materials were screened for their ability to resist bacterial attachment. Following the initial fluorescence based screen for bacterial attachment, XPS, ToF-SIMS, FTIR and WCA were used to character material arrays and correlate bacterial attachment to material polarity. [83] Beyond material characterization, common medical devices were coated, implanted into rats, and their ability to resist bacterial attachment within an organism was evaluated. Depending on the parameters and desired outcome, it may be possible to identify material trends with a desired outcome. Regardless, combining material characterization

techniques offers a starting point or lead to more focused HTS for the production and development of microarray application.

1.7. Thesis Goals

In recent years, methodologies in combinatorial chemistry (CombiChem) and high throughput screening (HTS), applied by pharmaceutical companies for drug discovery, have been used in material science. Within material science, HTS has allowed the development of novel materials, as well as fine-tuning and optimization of existing materials for specific applications. Most notably is the use of HTS for the fabrication and identification of biomaterials *ie:* a material that incorporates biologically active entities.

The entrapment and characterization of biomolecules within inorganic silica materials has received a lot of attention. In part, due to the observed increased in biomolecule stability upon entrapment, and the sol-gel process itself, which can be carried out under mild conditions *ie:* low temperature and physiological pH. The research however is limited to the characterization of materials/assays on an individual basis. Few groups have utilized the power of HTS methods, such as microarrays, for the evaluation of sol-gel derived materials with a wide diversity in chemical composition on a single substrate. Those include work from Kim *et al.* who screened 100,000 sol-gel derived material combinations for the entrapment of proteins, antibodies and small molecules.[25] Another example from Monton et al. highlights a similar microarray based screen using a factorial based design to screen a specific subset of materials from a

possible 20,000 unique material combinations. [15] Indeed, both groups were able to identify a narrow range of materials optimal for the targeted bioassay. However, a very limited characterization into understanding the material-biomolecule interface/interaction was performed. Questions that offer explanation of the observed trends still remain unanswered.

Similar work from the group of Robert Langer investigated the use of polyacrylyte materials for the various applications including materials which resist/promote bacterial attachment. [21,22,85] Building off this existing microarray technology, work by Hook et al subsequently characterized the 576 unique polyacrylye based materials in microarray format. [83,84] The use of combining surface characterization techniques as XPS, AFM, TOF-Sims and WCA was the first example using multiple complex analysis methods to gain a better understanding of the material-biomolecule interaction on a microarray.

Considering the success of work initialed by the Alexander group, the overall goal of this thesis was HTS and surface characterization of sol-gel derived material microarrays. First, building on existing microarray technology previously completed within the Brennan group, material characterization using XPS and FTIR in both conventional and imaging modes on microarrays prepared following the fabrication techniques outlined in Monton *et al.* [15] Both XPS and IR were chosen as methods for array characterization to gain a better understanding of the chemical composition of the sol-gel derived materials. As novel work within the material field with respect to characterization of sol-gel derived microarays,

fundamental knowledge related to the material-biomolecule interface using characterization techniques mentioned above hope to identify possible trends in material-biomolecule activity. Furthermore, surface characterization combined with pre-existing fluorometric enzyme based assay will offer correlations between material chemistry and assay performance.

Expanding on microarray technology within the Brennan group, the utility of piezoelectric printing methods for the fabrication of sol-gel derived material microarrays was explored. While methods of array fabrication are discussed in detail below, briefly, piezoelectric printing expands the range of printable materials to cover a larger chemical space. Initially, work will focus on the direct comparison of arrays fabricated following pin printing methods in previous work, the long term goal beyond this individual thesis is a combinatorial HTS and surface characterization of sol-gel derived materials using piezoelectric printing methods. The in depth surface evaluation of materials in HT will allow a better understanding of key questions related to material-biomolecule interaction, activity and performance.

Chapter - Two | Experimental

2.1. Materials and Reagents

D-sorbitol, D-(+)-trehalose dihydrate, Triton™ X-100, Glycerol anhydrous, N_ε-Acetyl-L-lysine, trimethoxymethylsilane (MTMS, ≥ 98%), 3-aminopropyl-trimethoxysilane (APTES, 97%), poly(vinyl alcohol) (PVA, M_w 9,000-10,000, 80% hydrolyzed), poly(ethyleneimine) (PEI, M_w 1,300, 50 wt. % in H_2O), poly(ethylene glycol) (PEG, Mw 600), DOWEX® 50WX8 hyrdogen form (50-100 mesh), tetramethyl orthosilicate (TMOS, ≥ 99%), acetylcholinesterase (AChE) from *Electrophorus electricus* (EC 3.1.1.7), acetylthiocholine iodide (ATCh), 4-(2-hydroxyethyl)piperazine-1-ethanesulfonic acid (HEPES), tris(hydroxymethyl)aminomethane (Tris), ammonium hydroxide solution (25% in H_2O) and hydrogen peroxide solution (30 wt% in H_2O) were purchased from Sigma-Aldrich. BODPIY® FL L-Cystine was obtained from Invitrogen life technologies. N-(3-triethoxysilpropyl)gluconamide (GLS, 50% in EtOH), and carboxyethylsilanetriol (Si-COOH, 25% in H_2O) were purchased from Gelest. Sodium silicate solution (29.2% SiO_2, 9.1% NaO, 61.7% H_2O) was purchased from Fisher Scientific, and diglycerylsilane (DGS) synthesized following the procedure as described elsewhere, [53] and confirmed with Si^{29} NMR. All water used was double distilled (ddH_2O) and obtained from a Milli-Q Advantage A10 water purification system (EMD Millipore, Billerica, MA).

2.2. Sol Precursor Preparation

Sodium silicate based sols (SS) were prepared from sodium silicate solution and charged DOWEX®. Briefly, DOWEX® was charged with 0.1N hydrochloric acid (HCl) and washed with ddH_2O until the filtrate was clear. In a 50 mL plastic beaker, 2.59 g of sodium silicate solution were mixed with 10 mL of ddH_20 and 5.6 g of charged DOWEX®. The solution was stirred vigorously for two minutes then vacuum filtered using Whatman® 44 filter paper. The sol was further filtered through a 0.2 µm syringe filter, stored in ice, and referred to as 100% SS.

DGS based sols were prepared first by crushing ~ 1 g of crystalline diglycerylsilane using a mortar and pestle. The crushed diglycerylsilane was then hydrolyzed at 1 g/mL and sonicated in ice for 20 minutes and mixed for 5-second intervals on a vortex every 5 minutes. The sol was filtered through a 0.2 µm syringe filter, stored in ice, and referred to as 100% DGS.

TMOS based sols were prepared by mixing TMOS, ddH_2O, and HCl (0.1 N) in a 6.9:93.1:0.002 molar ratio. The resulting solution was mixed for 30 seconds by vortex and sonicated on ice for 20 minutes. Following sonication, the sol was used immediately or further mixed using a magnetic stir bar for 24 hours. The sol was further filtered through a 0.2 µm syringe filter and referred to as 75% TMOS.

2.3. Additive Preparation

Various small molecules, organosilane and polymer additives were prepared as aqueous solutions in ddH_2O. Small molecule stock solutions of sorbitol, trehalose and lysine were prepared at 2 mM and 3 mM, Triton™ X-100 at 1 mM and 1.5 mM, and glycerol at 40% and 60% (v/v). Polymer solutions of PVA and PEI were prepared at 8%, 16% and 24% (w/v) and PEG as 40% and 60% (w/v) stock solutions and required sonication to assist pellet dissolution. Stock organosilanes GLS, Si-COOH and MTMS were prepared at 16% and 24% (v/v) solutions miscibility. All additives solutions were stored at 4 °C and used for up to one month with the exception of lysine that was required to make fresh solution before each use.

2.4. Material Formulations

Material formulations were prepared according to Table 2.1 by mixing the various additives together in the well of a 384 microtiter plate. Formulations always contained by volume, 25% combined additives, 55% buffer and 20% enzyme solution at two times the desired final concentration. Generally, a 25 µL total solution was prepared; with formulations containing 2 additives, 3.13 µL of each additive was used and when formulations contained 3 additives, 2.08 µL of each additive was combined along with 13.74 µL of 50 mM HEPES, pH 8.0 and 5 µL of a 2 KU/mL solution of AChE in 50 mM Tris, pH 8.0.

Table 2.1**:** Material combinations for the entrapment and characterization of AChE microarrays. Various additives are listed along with their final concentration when mixed 1:1 with the sol.

Material #	Sol*	Additive-1	Additive-2	Additive-3
1	DGS	Sorbitol, 125 µM	ddH_2O	
2	DGS	Glycerol, 2.5%	ddH_2O	
3	DGS	Si-COOH, 1%	ddH_2O	
4	DGS	GLS, 1%	ddH_2O	
5	DGS	GLS, 1%	Sorbitol, 125 µM	
6	DGS	GLS, 1%	Trehalose, 125 µM	
7	DGS	GLS, 1%	Glycerol, 2.5%	
8	DGS	PVA, 0.5%	Sorbitol, 125 µM	
9	DGS	PVA, 0.5%	Glycerol, 2.5%	
10	DGS	PVA, 1%	Sorbitol, 125 µM	
11	DGS	PVA, 1%	Glycerol, 2.5%	
12	DGS	PVA, 1%	GLS, 1%	
13	DGS	PVA, 1%	GLS, 1%	Sorbitol, 125 µM
14	DGS	PVA, 1%	GLS, 1%	Triton X100, 62.5 µM
15	DGS	PVA, 1%	GLS, 1%	Trehalose, 125 µM
16	DGS	GLS, 1%	Lysine, 125 µM	
17	DGS	Lysine, 125 µM	ddH_2O	
18	DGS	Si-COOH, 1%	Triton X100, 62.5 µM	
19	DGS	Si-COOH, 1%	Lysine, 125 µM	
20	SS	PVA, 1%	Glycerol, 2.5%	
21	DGS	ddH_2O	ddH_2O	
22	DGS	GLS, 1%	Triton X100, 62.5 µM	
23	DGS	PVA, 0.5%	ddH_2O	
24	DGS	PVA, 0.5%	Trehalose, 125 µM	
25	DGS	PVA, 0.5%	Triton X100, 62.5 µM	
26	DGS	PVA, 1%	ddH_2O	
27	DGS	PVA, 1%	Trehalose, 125 µM	
28	DGS	PVA, 1%	Triton X100, 62.5 µM	
29	DGS	PVA, 1%	GLS, 1%	Lysine, 125 µM
30	DGS	PVA, 1%	GLS, 1%	Glycerol, 2.5%
31	DGS	PVA, 1%	Lysine, 125 µM	
32	DGS	PEG, 3.75%		
33	DGS	PEG, 7.5%		
34	SS	PVA, 0.5%	ddH_2O	
35	SS	PVA, 1%	ddH_2O	

*Prepared sols as per section 2.2 mixed 1:1 with ddH_2O before adding 1:1 with the buffered-AChE-additive solution.

2.5. Microarray Formation

Microarrays were either fabricated by contact pin-printing or non-contact piezoelectric inkjet methods on amine derivative slides. For enzymatic microarray characterization. commercially purchased amine coated slides (Arrayit®) were used. All remaining methods of microarray characterization (XPS, FTIR and MALDI-MS) required a reflective and/or conductive surface. As such, 1000 Å gold coated slides (Sigma-Aldrich) were coated with an amine derivative following a modified procedure as described by Wang *et al.* [86] Briefly, the gold slides were cleaned using a basic piranha solution (5:1:1, ddH_2O:ammonium hydroxide (25% v/v):hydrogen peroxide (30% v/v)) heated to 75 °C following 10 minutes within a ultraviolet (UV)/ozone chamber. When no residual matter could be seen visually, the slides were immersed into a ddH_2O bath for 5 minutes followed by 95% (v/v) ethanol (EtOH). Slides were subsequently immersed into a coating solution of 0.5 mM 11-amine-1-undecanthiolthiol hydrochloride in anhydrous EtOH. Prior to printing, the desired number of slides were removed from the coating solution and immersed into 95% EtOH before being dried under a stream of nitrogen. Slides were stored for up to two weeks within the coating solution.

2.5.1. Contact Pin-printing

A Virtek Chipwriter Pro® (Bio-Rad Laboratories, Missauga, ON) contact pin-printer was used to print the various spotting solutions. Spotting solutions were composed of a 1:1 mixture of the various material formulations prepared in

section 2.4 and the respective sol noted in Table 2.1. Each spotting solution was prepared by adding the respective sol to the additive solution prior to the printing pin lowering within the sample. For material spot deposition the print head was equipped with a single SMP7 stealth pin (Arrayit, 250 nL uptake volume; 2.3 nL delivery volume; 235 µm spot diameter) and control over all printing parameters was done through the Chipwriter Pro (CWP) software. Briefly, travel in the XY plane was set to 10 mm/s and sample approach speed set at 2 mm/s with a 3-second dwell time and ~1-second contact time. All printing was carried out within a printing chamber at 23 ± 2 °C and a minimum of 85% relative humidity. After spotting each solution, the print run was paused; the printing pin was removed, cleaned and rinsed using ddH_2O and dried prior to subsequent spotting.

2.5.2. Non contact Piezo-inkjet printing

A sciFLEXARRAYER 5 (S5, Scienion US, Monmouth Junction, NJ), piezoelectric printer was used to evaluate non-contact printing methods for fabricating sol-gel derived material microarrays. Solutions were spotted using various piezoelectric dispensing capillaries (PDC) of variable size (40-80 µm diameter nozzle orifice) and coating (PDC coating type-4, Scienion). Control over all spotting parameters including voltage (V), pulse width (µs), frequency (Hz), camera parameters including strobe delay (µs), and nozzle cleaning conditions including flush volume, time and sonication were done through the accompanying software (sciFLEXARRARYER V 8.11). Methods for optimizing and printing

spotting solutions are described in detail as part of the results and discussion section. For material deposition, a minimum of two PDC nozzles were used; one which contained the desired sol and remaining PDC's that contained the various material additives (polymer, organosilane or small molecule), buffer and enzyme solution separately (4 PDC nozzles in total) or premixed (2 PDC nozzles in total). The use of multiple nozzles allowed the various required solutions to be spotted subsequently one after another (drop-on-drop) allowing *in situ* formation of the sol-gel derived materials. Prior to printing, systems water was obtained by degassing fresh vacuum filtered (0.2 μm membrane filter) ddH_2O. Furthermore, the system water level was maintained equal to the height of the printing stage. This ensured the printer was operating at maximum efficiency.

2.6. Microarray Characterization

Following successful printing experiments using either contact or non-contact printing methods, the resulting microarrays were assed using various methods of characterization mentioned below. The methods described within this section are ordered to reflect the actual workflow designed to evaluate microarrays in succession of one-another and reduce the number of produced arrays required for characterization. For XPS, and FTIR characterization, printed microarrays were submitted to the Biointerfaces Institute at McMaster Univeristy, Hamilton, Ontario

2.6.1. Optical microscopy

Optical images of printed arrays were collected using an Olympus BX53 brightfield/fluorescence microscope equipped with a X-Cite® (120Q series, Lumen Dynamics) illumination system and a 12 bit monochromatic CCD camera (Retiga 2000R, Qimaging). Microarrays were imaged to assess spot deposition (uniformity, cracking, material homogeneity). Fluorescence images of spotting solutions containing 50 µM fluorescein were taken to confirm spot-ability with the S5 printer.

2.6.2. Enzymatic activity

The enzymatic activity of AChE was evaluated using a fluorometric assay as described elsewhere. [15] Briefly, the substrate acetythiocholine in the presence of AChE generates free thiochlone for the sulfide-thiol exchange reaction of the intramoleculary quenched dimeric BODIPY-FL-L-cystine dye. For on-array activity, positive control (PC) and negative control (NC) solutions were over-spotted onto existing sol-gel derived material arrays using a SMP10XBstealth pin of larger diameter (Arrayit, 1,250 nL uptake volume; 6.9 nL delivery volume; 400 µm spot diameter). The PC solution contained a final concentration of 500 µM ATCh and and 14 µM BODIPY-Fl-L-cystine in 25 mM Tris, pH 8.0, with 4% glycerol while the NC solution was prepared without the substrate, ATCh. For each material, a minimum of 25 replicates for both the PC and NC were used to determine the enzymatic activity. Over-spotted microarrays were aged for a

maximum of 1 hour within an enclosed chamber at room temperature (23 ± 2 °C) and a minimum of 85% relative humidity. Slides were imaged using a NovaRay imager (Alpha Innotech) with a white light source and CCD detection system equipped with a 478 ± 17 nm excitation and 538 ± 21 nm emission filter. Microarray images were acquired at a minimum resolution of 4 μm and automatic excitation and emission exposure settings. The resulting intensity for each spot was calculated using ImageJ and reported as the intensity minus the blank slide background.

2.6.3. Infrared Microscopy

An IR spectrum from printed microarrays was obtained using a Hyperion 3000 (Bruker) FTIR microscope run in reflectron mode and equipped with OPUS 7.2 operating software. Single point spectra were collected from 3000 to 500 wavenumber (cm^{-1}) using the 15× optical objective to focus the sample. Prior to acquiring sample spectra, a background scan was collected, reported (average of 64 scans) and automatically accounted for within the software. When performing multi-point spectra analysis, added background scans were performed after every 5-sample points. Reported sample point scans were also the average of 64 individual scans.

2.6.4. X-ray Photoelectron Spectroscopy (XPS)

Characterization was completed on a PHI Quantera II XPS scanning microprobe (Physical Electronics (Phi), Chanhassen, MN) equipped with a 1486.7 eV monochromatic Al-K-alpha X-ray source. All settings were controlled through supplied software (Multipak 9.4.0.7) and the system was run to collect single point spectra (survey spectra) and various forms of maps. Survey spectra were collected using a beam size of 200 µm and a 280 eV pass energy, while small image maps used a 50 µm beam size and 280 eV pass energy and large image maps used a 100 µm beam size, 280 eV pass energy and set up to get a pixel size of 100 µm.

2.7. Bio-ink Formulation

Select additive solutions were tested for their viscosity, surface tension and particle size to better understand their printability using the S5 non-contact printer.

2.7.1. Surface Tension

Surface tension measurements were performed with a high-speed Optical Contact Angle (Future Digital Scientific, Garden City, NY) instrument. All measured solutions were prepared at room temperature (23 ± 2 °C) and prior to measurement acquisition 500 µL of each solution was manually flushed through the system lines. Solution specific acquisition was controlled through the supplied software, SCA 20. Briefly, a 2.04 mm diameter fixed needle was

brought into manual focus and solution was dispensed creating a hanging pendant-drop. For each solution, the volume dispensed was the maximum volume that could withstand gravimetric forces. The resulting surface tension (interfacial tension (IFT), mN/m) was calculated through the software fitting the Laplace-Young equation (Equation 1); where p, γ, R1 and R2 represent pressure, surface tension and the principal radia above (R1) and below (R2) the curvature of the drop.

$$\text{Equation 1: } \Delta p = \gamma \times \left(\frac{1}{R1} + \frac{1}{R2}\right)$$

2.7.2. Viscosity

The viscosity of various additive solutions was determined by a tuning-fork vibration viscometer (SV-10, Vibro Viscometer, A&D Instruments, Oxford UK). Viscosity measurements required a minimum sample volume of 10 mL and height adjusted such that the solution level just covered the instrument paddles. Prior to testing, the viscometer was calibrated following the one-point calibration method using ddH_2O. Briefly, the temperature dependent viscosity of ddH_2O was determined and adjusted according to the instrument table provided. The absolute viscosity (mPa*s) of each solution was calculated using the resulting displayed viscosity following equation 2.

$$\text{Equation 2: } \text{Absolute viscosity } (\text{mPa} * \text{s}) = \frac{\text{Displayed viscosity (mPa*s)}}{\text{Sample Density (g)}}$$

2.7.3. Dynamic Light Scattering (DLS)

The particle size distribution of various sols (DGS, SS and TMOS) were determined by dynamic light scattering using a Zetasizer Nano ZS (Malvern Instruments, Worcestershire UK) equipped with non-invasive backscatter (NIBS) optics. Particle size measurements were determined using a red laser (633 nm) collecting backscatter at 173°. Samples were run using disposable polystyrene cuvettes filled with 1-1.5 mL of sample and the resulting data was plotted as intensity % versus particle size diameter (nm).

Chapter - Three | Results and Discussion

3.1. Characterization of Pin-Printed Sol-Gel Derived Microarrays

Previous work within the Brennan group assessed the utility of sol-gel derived materials for developing bio-encapsulated microarrays using a contact pin-printer. [58,59] This method identified a small subset of materials that first example using a guided material screen approach to systematically reduce the large number of factorial material combinations. [15] However, array characterization was limited to the determined on-array enzyme activity and ranked by category of optimal and non-optimal materials. Optimal materials were defined by a positive control (PC) to negative control (NC) ratio greater than three. The aim of this work was to provide further insight as what in the amterial could be responsible/explain the differences in activity. From the above-mentioned work, 35 unique sol-gel derived material formulations (Table 2.1), 20 optimal and 15 non-optimal, i.e. PC/NC ratio > 3 when printed onto an amine coated slide surface, were chosen for array characterization by X-ray photoelectron spectroscopy (XPS) and infrared spectroscopy (IR).

3.1.1. Elemental Surface Characterization using X-ray Photoelectron Spectroscopy (XPS)

From pin-printed arrays of the select 35 unique material formulations, single point spectra were collected and analyzed for their relative elemental

atomic composition. For each unique material composition, acquired XPS surface characterization was plotted against their experimentally determined PC/NC ratio (Figure 3.1).

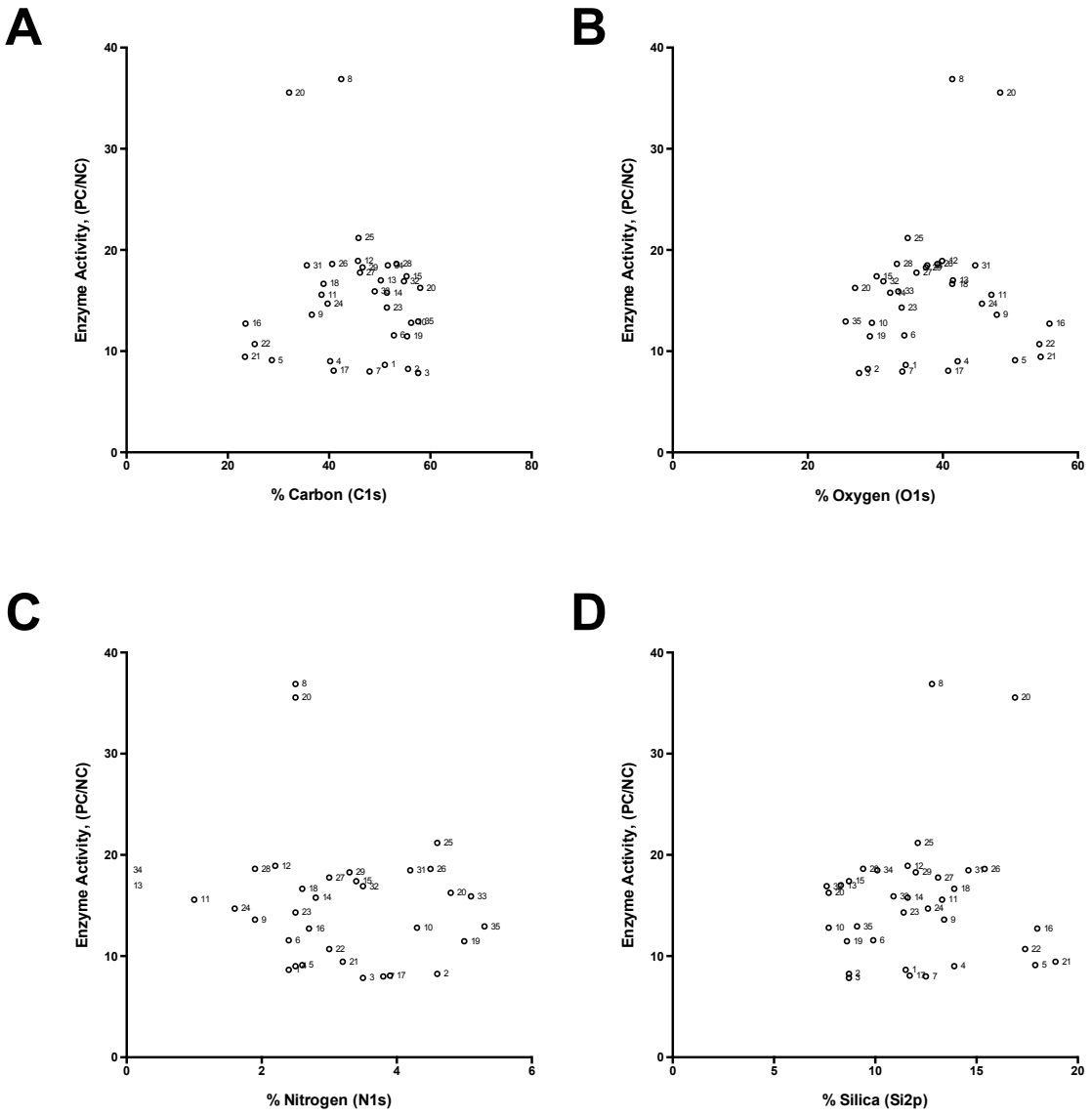

Figure 3.1: Comparison between elemental composition of on-array sol-gel derived materials determined by X-ray photoelectron spectroscopy against enzyme activity for A) carbon, C1s, B) oxygen, O1s, C) nitrogen, N1s and D) silica, Si2p.

With respect to surface concentration of oxygen (O1s), carbon (C1s), nitrogen (N1s) and silicon (Si2p), there was no observed correlation between elemental percentage and observed enzymatic activity. For elements such as carbon, oxygen and silica, this was not surprising as the unique material formulations were simply different mixtures of the same additive solutions pre-combined and mixed 1:1 (v/v) with either SS or DGS based sols of ~ 5.6 wt% and 5 wt% silicon respectively.

Perhaps, the most interesting observation was the lack of correlation between the nitrogen atomic percent and enzymatic activity. With only two additives, Nε-Acetyl-L-lysine and GLS containing elemental nitrogen, the main source of nitrogen remained AChE itself. It was hypothesized that materials with a greater observed enzymatic activity would have more surface available protein and, thus, a higher percentage of elemental nitrogen. Comparing material formulations with nitrogen containing additives to materials where the only known source of nitrogen was from the protein itself, both groups of materials contained similar amounts (0.7 ± 0.05 %) of elemental nitrogen. To further conclude, the different types of nitrogen bonds needed to be determined. Attempts to do so were done using XPS, but the data was not conclusive.

Elemental surface composition of materials prepared in a microarray format was also compared to bulk, hand-spotted arrays of similar materials (Figure 3.2). For each respective element, oxygen (O1s), carbon (C1s), nitrogen (N1s) and silicon (Si2p), the compared array to bulk atomic percentage showed

little to no correlation with respective slopes of 0.7, 0.4, -0.3 and 0.3 and all with an R^2 of less than 0.2. A beam size of < 100 µm was selected to ensure only material and no background scatter from the slide would be measured.

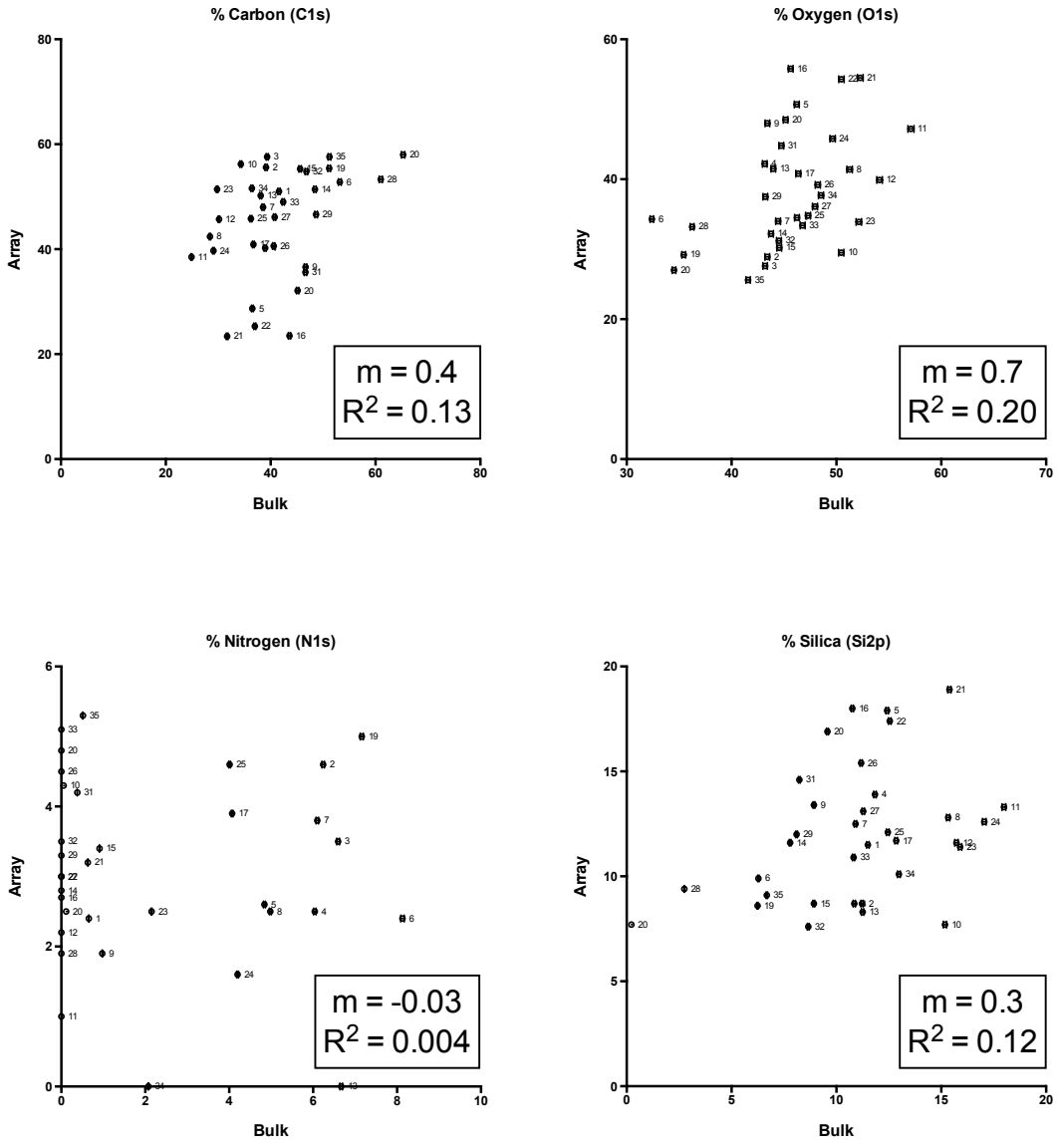

Figure 3.2: Comparison between elemental compositions of pin-printed sol-gel derived materials against hand-spotted "bulk" material arrays determined by X-ray photoelectron spectroscopy for carbon (C1s), oxygen (O1s), nitrogen (N1s) and silica (Si2p).

For each element, the formed array compositions seemed to differ from the bulk material. The observed difference in surface elemental composition was likely due to the difference in material dryness of pin-printed (~ 2.3 nL/spot) to hand-spotted (~ 3 µL/spot) materials. Both pin-printed and hand-spotted arrays were aged at room temperature for 4 days prior to XPS analysis. Attempts to age hand-spotted arrays longer resulted in severe material cracking and, as a consequence, compromised material adhesion to the slide surface. As a result, bulk versus pin-printed arrays did not contain the same water content, which influence the gelation kinetics and thus the gel composition *ie.* degree of cross linking and particle size. Determining the various types of silica specie *ie.* Si-O-Si or Si-OH, the degree of material specific cross-linking may be measureable. It may then be possible to correlate the degree of material cross linking to pore hydration and thus entrapped AChE activity.

Following conventional point spectra analysis, a high resolution spatial element map of carbon (C1s), oxygen (O1s), nitrogen (N1s) and silicon (Si2p), was acquired by XPS in imaging mode (Figure 3.3).

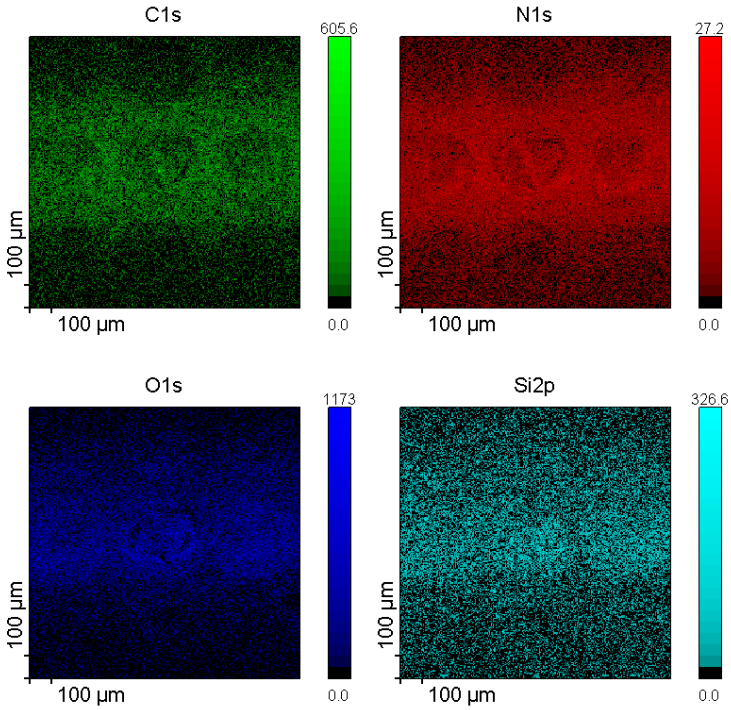

Figure 3.3: Various high resolution element maps from a section of a pin-printed sol-gel derived microarray by X-ray photoelectron spectroscopy (XPS). For visualization, false colouring (green – carbon, red – nitrogen, blue – oxygen, and aqua – silicon) was applied based on intensity where black was negligible.

As seen in Figure 3.3, while typically array patterns can be visualized through mapping elemental location, poor spot resolution was observed due to a higher than expected background signal of the blank slide. In order to achieve greater spot-to-spot resolution, future work requires the use of distinctively different slide surfaces such as gold. With greater resolution, it may be possible to use XPS mapping as a method for determining protein location within the surface of each material.

3.1.2. Chemical Characterization using Infrared Spectroscopy (FTIR)

Complimentary to XPS surface characterization, pin-printed sol-gel based microarrays were additionally characterized using infrared spectroscopy (IR) as a means to better understand AChE-material trends. Similar to XPS characterization, single point IR spectra (Data not shown) were obtained from 3000 to 500 cm^{-1} for the 35 select materials. Resulting spectra were subsequently analyzed by integrating the peak area from 1690 to 1600 cm^{-1} (Figure 3.4) and 1600 to 1500 cm^{-1} (Figure 3.5) for each material. Subsequently, the resulting absorbance at the peak maxima, 1655 cm-1 (Figure 3.4) and 1548 cm^{-1} (Figure 3.5) was plotted for each material. Ranges in wavenumber were select based on the known broad double peak IR spectra of proteins in H_2O with the former representative of the amide I band (C=O stretch) and the latter of the amide II band (N-H bending and C-N stretching) from side chain amino acids. [87] Extrapolation of the suspected amide I and amide II IR bands for protein alone did not provide insight towards material based performance.

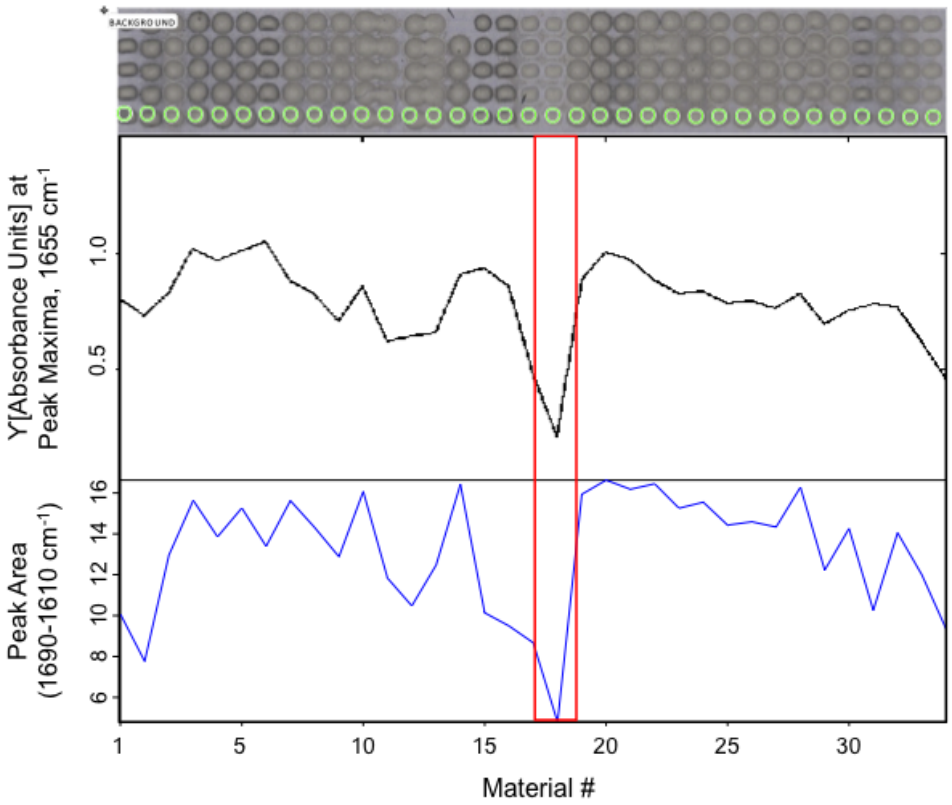

Figure 3.4: Representative spectra collected from a pin-printed array of 35 sol-gel derived materials (top) plotted according to integrated peak area from 1690 to 1610 cm^{-1} (bottom) and their resulting absorbance maxima at 1655 cm^{-1} (middle).

However, there was an observed correlation between the peak area from 1690 to 1610 cm^{-1} and the absorbance at peak maxima 1655 cm^{-1} in contrast to no correlation between the peak area from 1600 to 1500 cm^{-1} and the absorbance at peak maxima 1548 cm^{-1} highlighted with material 18 in both Figure 3.4 and Figure 3.5. This suggested the use of IR to discriminate entrapped AChE within sol-gel derived materials is not possible due to low protein concentrations and is in fact attributed to the various material additives.

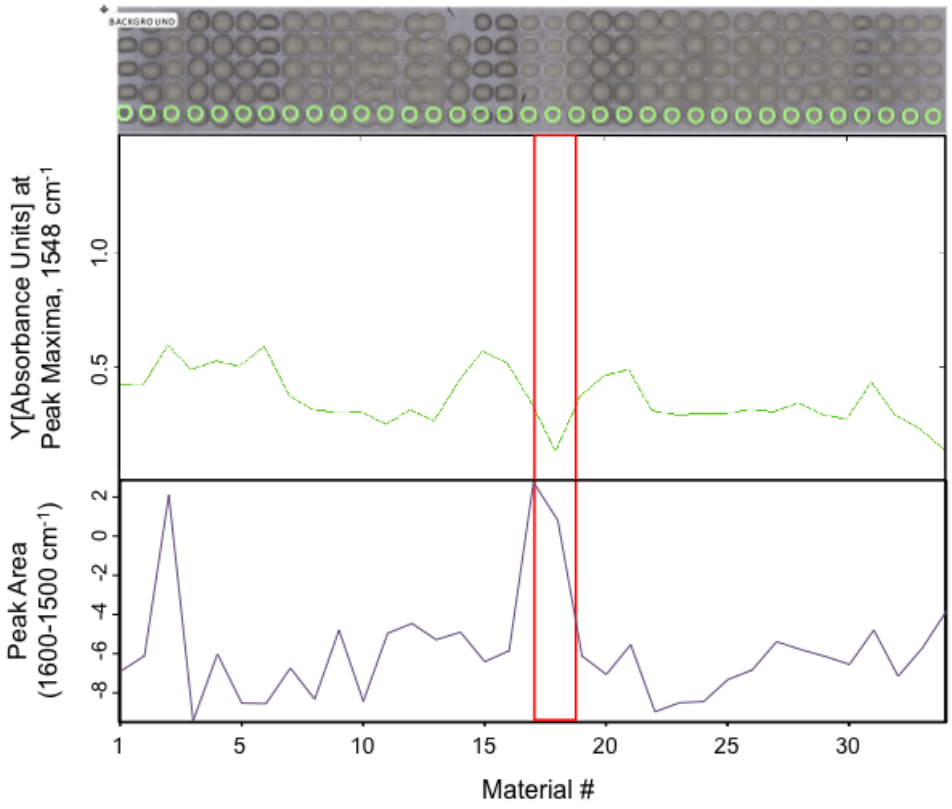

Figure 3.5: Representative spectra collected from a pin-printed array of 35 sol-gel derived materials (top) plotted according to integrated peak area from 1600 to 1500 cm^{-1} (bottom) and their resulting absorbance maxima at 1548 cm^{-1} (middle).

In addition to single point spectra, a chemical image of the array was additionally collected using the focal plane array detector with 2.7 μm resolution. Figure 3.6 shows the resulting high-resolution array image of the first five materials with applied color based intensity from the absorbance at 1655 cm^{-1} integrated over the acquired optical image.

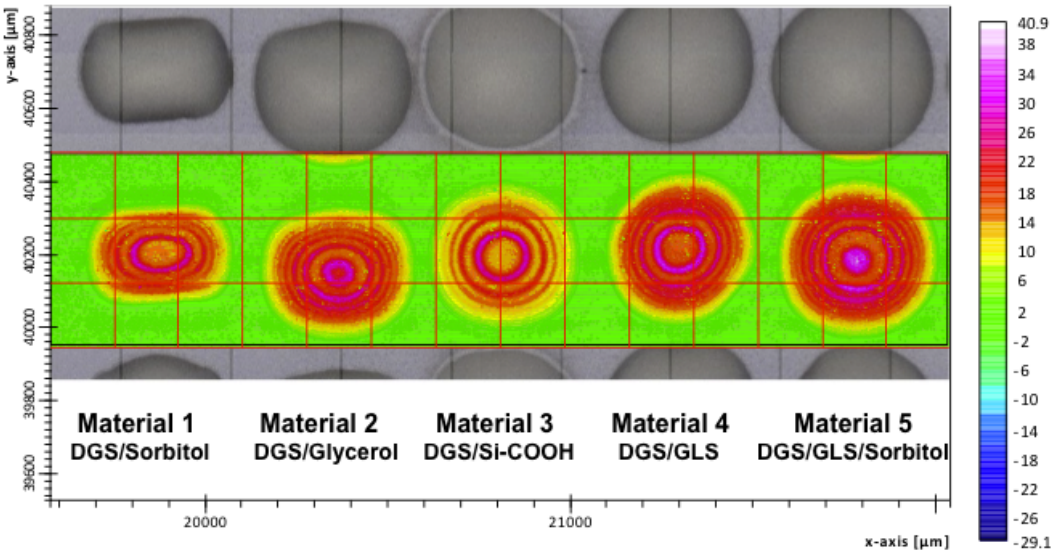

Figure 3.6: Chemical Based Imaging of 5 select sol-gel derived material formulations showing color based intensity collected at 1655 cm^{-1} using infrared spectroscopy (IR) equipped with a focal plane array (FPA) detector with 2.7 µm resolution.

With respect to the collected chemical image in Figure 3.6, the grid overlay is representative of the distinct capture area defined by the 64×64 grid array of detectors used to acquire the image. From the high 2.7 µm resolution, greater chemical spatial information can be seen visually to gain a better understanding of material homogeneity. The spatial distribution of the absorbance at 1655 cm^{-1} suggests the acquired intensity is in fact location specific as seen in Figure 3.6 and greatly emphasized within material 3. Thus, future IR characterization of microarrays should utilize IR imaging methods appose to obtaining single point spectra.

Additionally, cluster based analysis using instrument software to normalizing each of the 35 material collected IR spectra within the fingerprint

region (1700 to 500 cm^{-1}) was performed to better understand material differences (Figure 3.7).

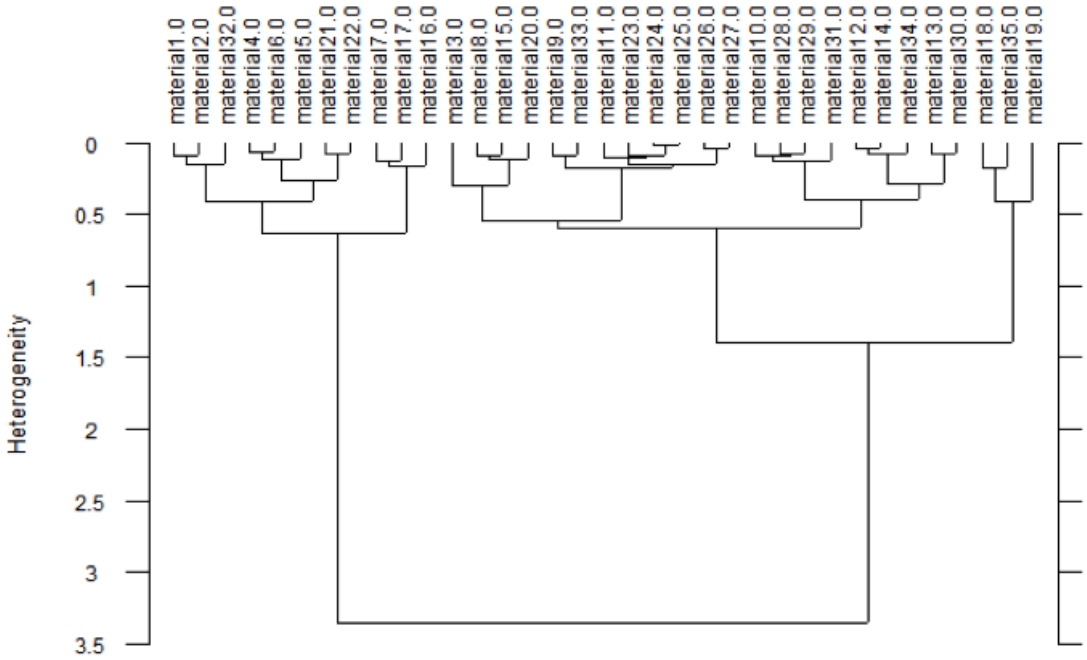

Figure 3.7: Material heterogeneity of 35 unique sol-gel derived material formulations produced with a contact pin-printer. Heterogeneity was based on cluster analysis of obtained IR spectra (1700 to 500 cm^{-1}).

From the resulting cluster analysis of the obtained IR spectra (1700 to 500 cm^{-1}), the widest degree of material similarity divided the materials into 2 groups. Of the largest group of materials shown on the right side of Figure 3.7, all but 2 compositions have poly(vinyl alcohol) (PVA) as a polymer additive while all materials within the second group have no material combinations containing

PVA. Moreover, of the material group with PVA, 50% were identified with optimal activity of entrapped AChE compared to 73% of the materials from the group lacking PVA that showed optimal AChE activity. However, given the material with the greatest PC/NC ratio was sodium silicate based with PVA and glycerol (Material 20) trends in material performance cannot be based solely on the obtained cluster analysis. To achieve a greater distribution of material clusters that may offer trends in material performance, a larger material pool is required.

3.2. Piezoelectric Inkjet Methods for Non-contact Microarray Fabrication

As a means to overcome the material limiting 2.5-hour gelation criteria required for contact pin-printing, microarray fabrication with a non-contact piezoelectric inkjet printer was investigated. In fact, in order to produce material arrays using a pin-printer, the 2.5-hour minimum gelation time reduced significantly the number of material formulations and the so-produced materials were assessed for the printability and ability to retain on-array enzyme activity. As such, of the possible 20,000 material formulations, only ~ 200, or 1 %, were actually spotted using the contact pin-printer.[15] Furthermore, the systematic material design excluded formulations based on the sequential addition of additive groups which resulted in material gelation < 2.5 hours regardless of possible further material additive interactions that may have altered gelation times enough to justify testing their printability. Consequently, the attraction of array fabrication using non-contact methods was favored due to high printing versatility and the ability to print each required additive from separate printing

reservoirs. This so-called drop-on-drop design would allow material formulation in situ and the potential to screen all 20,000 material formulations in a timely manner. Furthermore, it was hypothesized that this technique would identify a larger subset of materials that retained optimal activity of entrapped AChE.

Initial efforts with data shown below highlighted that a direct material comparison was not possible. Consequently, the second goal of this thesis to develop high density sol-gel derived material arrays using a non-contact printer shifted to bio-ink formulation to better understand and explore the limitations of piezoelectric inkjet printing for fabrication of sol-gel derived material arrays.

3.2.1. Bio-ink Formulation for Non-contact Piezoelectric Inkjet Printing

Focusing solely on understanding parameters that both controlled and limited the S5 non-contact piezoelectric printer, all solutions were compared for spot-ability using piezoelectric dispensing capillaries (PDC) of varying orifice diameter (PDC80, 80 μM diameter orifice, PDC60 and PDC40) with and without a select proprietary inner capillary coating (Type 4) to facilitate the spotting of silica based sols. Prior to spotting select material arrays, each independent solution-PDC combination required optimization to ensure stable spots were produced (Figure 3.8A and Figure 3.8B).

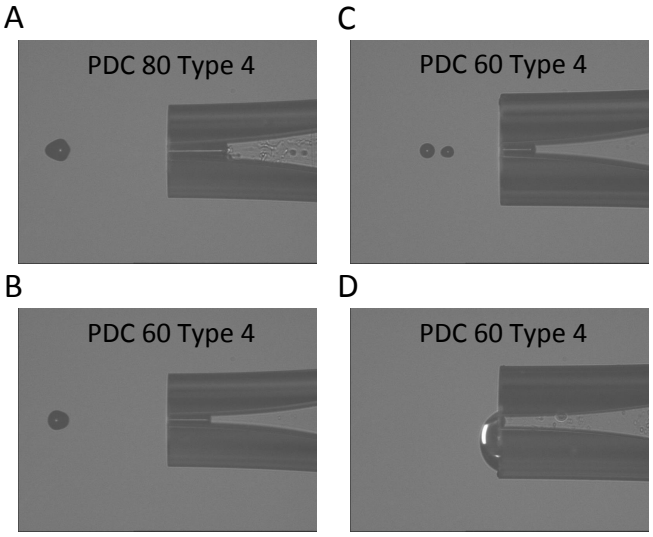

Figure 3.8 Composite of various spot images produced using a piezoelectric printer highlighting variable optimal drop shape with nozzle size (A and B), optimal versus non-optimal spotting from the same nozzle (B and C) while spotting ddH_2O and a non spot-able solution (D) glycerol.

By changing the applied voltage and pulse, the drop speed and volume for a given solution could be altered. While, in theory, the voltage and/or pulse could be adjusted to produce equal drop volumes for different spotting solutions, this often resulted in non-stable spots with satellite drops (Figure 3.8C). In some cases, solutions were not spot-able at all (Figure 3.8D) and often resulting in clogged nozzles. This was first observed with initial efforts that focused solely on the printability of select sols prepared from SS and DGS. The respective sols were prepared in a way that the final silica content was 5.6 wt% and 5.0 wt% for SS and DGS. Attempts to print the sols prepared as is was unsuccessful and led to compromised nozzles due to clogging.

To assess the possibility of drop-on-drop array fabrication methods, increasing concentration of additives solutions including polymers (PVA, PEI and

PEG), organosilanes (GLS, MTMS, APTES and Si-COOH), small molecules (sorbitol, trehalose, glycerol, Triton X-100 and lysine), and silane precursors (SS, DGS and TMOS), were evaluated for their individual printability. Additionally, solution viscosity and surface tension were measured to identify trends and understand solution printability. Summary of solution printability compared to surface tension and viscosity is shown for small molecules (Table 3.1), organosilanes (Table 3.2), polymers (Table 3.3), and sols (Table 3.4).

The observed trend of increased viscosity with increasing solution concentration of polymer, organosilane, sol and glycerol solutions was expected. Similarly, it was also expected that the viscosity of trehalose, sorbitol, lysine and Triton remained constant even over a 10-fold concentration range. More importantly, comparing solution viscosity to printability (all solutions with the exception of the various prepared sols), only solutions with an observed viscosity of less than 5 mPa*s were printable. Surprisingly, the determined surface tensions for all additives were similar regardless of concentration.

Perhaps the most surprising result was that obtained for GLS. GLS solutions from 1 to 25 % v/v had respective viscosities of 1.08, 2.34 and 5.97 mPa*s and surface tension of 65.49, 62.98 and 32.19 mN/M (Table 3.2). While 25 % v/v GLS was not printable, this was unexpected given the almost 50% lower surface tension compared to 1 and 10 % v/v solutions. Although viscosity and surface tension are known variables that affect a given solution printability, and

given the fact that overall surface tension of observed printable additive solutions ranged from 30.75 to 71.72 mN/M and viscosities up to 5 mPa*s, solution viscosity has a greater influence on solution printability.

Table 3.1: Piezoelectric printability of select small molecule additives at various concentrations compared to viscosity and surface tension.

			Nozzle Printability		
Solution	Viscosity (mPa*s)	Surface Tension (mN/M)	PDC 80 Type 4	PDC 60 Type 4	PDC 40
1 mM Trehalose	1.01	71.35	ND	Yes	Yes
10 mM Trehalose	0.98	71.46	ND	Yes	Yes
1 mM Sorbitol	0.97	71.42	ND	Yes	Yes
10 mM Sorbitol	0.96	71.39	ND	Yes	Yes
1 mM Lysine	0.96	71.43	ND	Yes	Yes
10 mM Lysine	0.95	71.45	ND	Yes	Yes
1 mM Triton	0.95	31.09	ND	Yes	Yes
10 mM Triton	0.99	30.98	ND	Yes	Yes
10% v/v Glycerol	1.17	66.5	Yes	ND	ND
20% v/v Glycerol	1.82	ND	Yes	ND	ND
30% v/v Glycerol	2.47	ND	Yes	ND	ND
40% v/v Glycerol	3.95	ND	Yes	ND	ND
50% v/v Glycerol	7.16	60.92	No	ND	ND
60% v/v Glycerol	12.3	ND	No	ND	ND

ND = not determined

Table 3.2: Piezoelectric printability of select organosilane additives at various concentrations compared to viscosity and surface tension.

Solution	Viscosity (mPa*s)	Surface Tension (mN/M)	Nozzle Printability		
			PDC 80 Type 4	PDC 60 Type 4	PDC 40
1% v/v MTMS	1.01	46.77	Yes	ND	ND
10% v/v MTMS	1.37	42.12	Yes	ND	ND
25% v/v MTMS	2.24	30.75	Yes	ND	ND
50% v/v MTMS			No	ND	ND
1% v/v APTES	0.76	69.69	Yes	ND	ND
10% v/v APTES	1.38	59.61	Yes	ND	ND
25% v/v APTES	3.21	50.36	Yes	ND	ND
1% v/v GLS	1.08	65.49	Yes	Yes	ND
10% v/v GLS	2.34	62.98	Yes	Yes	ND
25% v/v GLS	5.97	32.19	No	No	ND
1% v/v Si-COOH	ND	70.01	ND	Yes	ND
24% v/v Si-COOH	ND	64.11	ND	Yes	ND

ND = not determined

While the printability of all polymer, organosilane and small molecules solutions utilized could be predicted by viscosity alone, this was not true for prepared sols. With respect to sodium silicate (SS) based sols, all dilutions prepared had viscosities of less than 2 mPa*s (Table 3.4). However, attempts to print any dilution were unsuccessful. A similar trend was observed for DGS based sols, which suggested piezoelectric inkjet printing methods were not applicable to aqueous based sols. While alkoxysilanes, such as TMOS, liberate free alcohol during condensation that can be detrimental to entrapped proteins, it is believed the alcohol might in fact reduce sol viscosity and facilitate their printability using a piezoelectric printer. However, despite TMOS solutions up to

70% which had viscosities less than 5 mPa*s, only TMOS solutions of up to 20% were printable. Therefore, the hypothesis that liberated alcohol, which would lower solution viscorty and aid in printing, is false. If this were in fact the true, sols of greater TMOS concentration would print with increasing difficulty at reduced concentrations.

Table 3.3: Piezoelectric printability of select polymer additives at various concentrations compared to viscosity and surface tension.

			Nozzle Printability		
Solution	Viscosity (mPa*s)	Surface Tension (mN/M)	PDC 80 Type 4	PDC 60 Type 4	PDC 40
1% v/v MTMS	1.01	46.77	Yes	ND	ND
10% v/v MTMS	1.37	42.12	Yes	ND	ND
25% v/v MTMS	2.24	30.75	Yes	ND	ND
50% v/v MTMS			No	ND	ND
1% v/v APTES	0.76	69.69	Yes	ND	ND
10% v/v APTES	1.38	59.61	Yes	ND	ND
25% v/v APTES	3.21	50.36	Yes	ND	ND
1% v/v GLS	1.08	65.49	Yes	Yes	ND
10% v/v GLS	2.34	62.98	Yes	Yes	ND
25% v/v GLS	5.97	32.19	No	No	ND
1% v/v Si-COOH	ND	70.01	ND	Yes	ND
24% v/v Si-COOH	ND	64.11	ND	Yes	ND

ND = not determined

Table 3.4: Piezoelectric printability of select sols at various concentrations compared to their observed viscosity and surface tension.

Solution	Viscosity (mPa*s)	Surface Tension (mN/M)	Nozzle Printability		
			PDC 80 Type 4	PDC 60 Type 4	PDC 40
5% SS	1.31	ND	No	ND	NA
10% SS	1.31	ND	No	ND	NA
15% SS	1.33	ND	No	ND	NA
25% SS	1.39	ND	/	/	NA
50% SS	1.51	ND	/	/	NA
100% SS	1.68	ND	/	/	NA
10% DGS	ND	ND	No	ND	NA
1% TMOS	1.09	ND	Yes	Yes	NA
15% TMOS	1.61	ND	Yes	Yes	NA
25% TMOS	1.91	ND	No	No	NA
50% TMOS	3.17	ND	No	No	NA
60% TMOS	3.9	ND	ND	ND	NA
65% TMOS	3.83	ND	ND	ND	NA
70% TMOS	4.09	ND	ND	ND	NA
100% TMOS	5.87	ND	ND	ND	NA

ND = not determined, NA = not applicable

3.2.2 Particle size Effects on Sol Spot-ability

To better understand the limitation of printing SS, DGS and TMOS based sols, the particle size distribution was determined using dynamic light scattering (DLS, Figure 3.9). Since select sol solutions were below the determined printable viscosity limit of 5 mPa*s, it was believed the various sol solutions contained silica particles capable of blocking the PDC nozzle orifice.

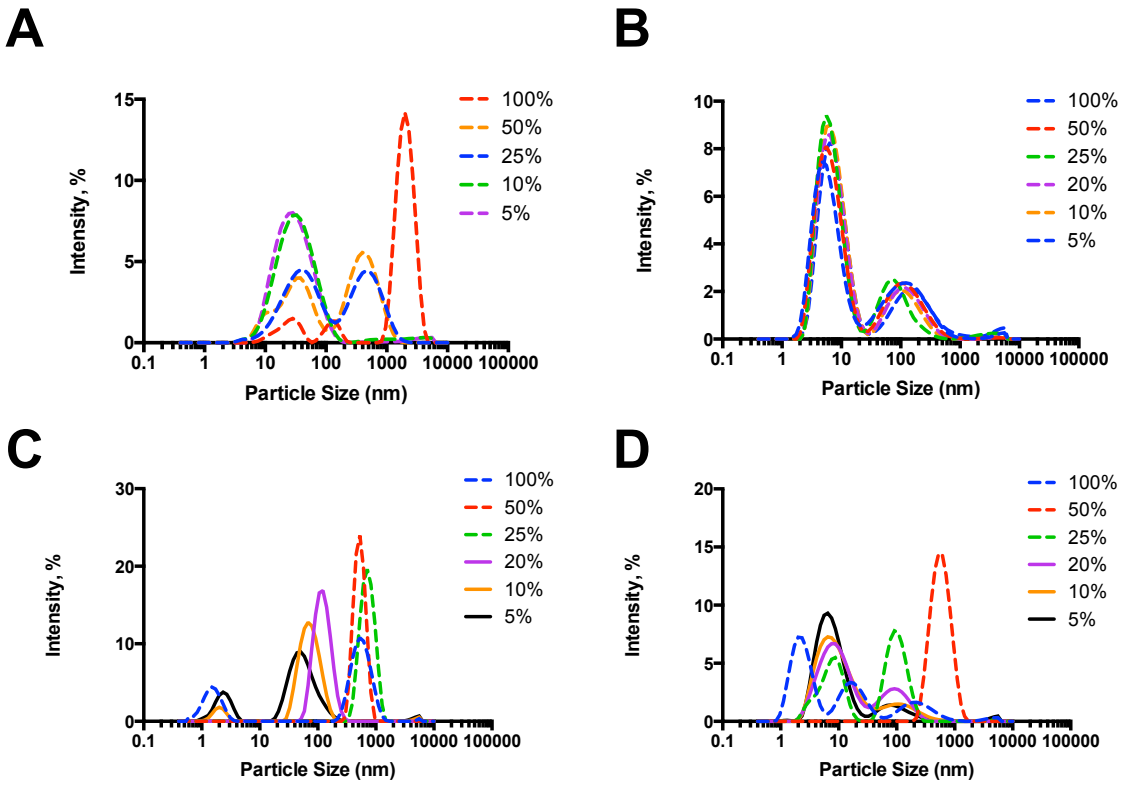

Figure 3.9: Various sol dilutions of sodium silicate (SS, A), diglycerylsilane (DGS, B), and tetramethylorthosilicate (TMOS) with varying hydrolysis time (0 hours, C and 24 hours, D) compared to solution particle size distribution. Printable sol solutions are represented by solid lines whereas dashed lines represent sols not printable by non contact piezoelectric inkjet printing methods.

The dynamic light scattering (DLS) instrument used was limited to detecting particles from 0.001 to 10 μm in diameter. While PDC nozzle diameters tested were from 40 to 80 μm, DLS measurements did suggest sol printability was limited by particle size. Of the observed particle size distribution, the observed peaks were likely primary particles and the further resulting particle populations due to aggregation. [46]

With respect to DGS based sols (Figure 3.9B), all dilutions showed similar particle size distribution profiles with two major particle populations of 10 and 100 nm in size. However, the profiles show relatively broad peaks. As such, sols were likely to contain particle aggregates up to 1000 nm.

Similarly, SS based sols (Figure 3.9A) show all dilutions with the exception of 5 and 10% SS to contain particles with a minimal size of 1000 nm. Comparing SS and DGS based sols to TMOS (Figure 3.9C), up to 20% TMOS show a maximum particle size of 100 nm and greater for increased TMOS concentrations. Given TMOS sols were printable up to 20%, the dynamic light scattering data suggest sols are printable as long as the particle population size remains less than 100 nm. The particle size distribution of similar TMOS sols was also measured following 24 hours of hydrolysis assuming complete TMOS hydrolysis. Interestingly enough, comparing particle size of each TMOS concentration after preparation and 24 hours (Figure 3.9D) shows a decrease in the intensity of larger particles and an increase in observed particles of smaller diameter. This would suggest preparing TMOS solutions 24 hours prior to printing would enhance the printing reproducibility due to the formation of more stable sols.

Further work exploring the use of different polymers and ionic strength to provide electrostatic stabilization of the resulting particles formed within the sol is needed to gain a better understanding on the effects of particle size and printability. It should also be noted that all sols tested for printability and used for

DLS measurements were prepared with a final pH of 4.0. While prepared TMOS based sols are known to be more stable from pH 2 to 3, the effects of acidity on the printing PDC crystal in unknown. Despite unknown PDC limitations, future work to identify stable sols with particle population's of minimal diameter (> 100 nm) may highlight a stable sol formulation that is amenable to piezoelectric inkjet printing methods.

Chapter - Four | Conclusions

Overall, this body of research was the first of its kind aimed towards better understanding observed differences in material formulations for the entrapment of biomolecules within select silica matrices following the sol-gel process. This was accomplished through the non-traditional use and evaluation of instrumental chemical characterization and aqueous based microarray printing techniques. Previously, work within the Brennan group established methods in contact pin-printing for the miniaturization and fabrication of high density sol-gel derived microarrays. Further work involved a systematic material screen to identify material trends which maintained acetylcholinesterase activity and additionally, the ability to perform high density quantitative assays on-array.

In an effort to better understand the observed material specific enzymatic activity, initial work focused on the characterization of select sol-gel derived materials microarrays fabricated using a contact pin-printer. Using X-ray photoelectron spectroscopy (XPS) and infrared spectroscopy (IR), these high information content methods were used in parallel (IR) and in sequence (XPS) to traditional fluorescence based imaging and characterization of printed arrays. Unfortunately, the results present within this body of work suggest the observed enzymatic activity can not be correlated to select material chemistry identified through independent assessment using either IR or XPS characterization techniques. Regardless, both methods, IR and XPS proved to be versatile and suitable techniques for the characterization of sol-gel based material microarrays.

However, perhaps a more substantial finding was the collective results obtained through IR chemical imaging. As a medium throughput technique, IR was especially useful for the assessment of spot-to-spot reproducibility and overall composition homogeneity. In fact, the observed difference in spatial distribution of suspected protein (amide I IR band at 1655 cm-1) suggests the materials are not smooth in nature. Thus, future characterization techniques should include the use of atomic form microscopy (AFM) to better visualize surface concavity.

Furthermore, the lack of observed material-enzyme activity correlations through XPS and IR characterization may have been directly related to the small subset of materials tested. While methods in piezoelectric printing were used in hopes of expanding overall material chemistry, efforts to directly compare the two method of array formation (contact pin-printing and piezoelectric ink jet printing) failed. Despite initial failure, an indirect understanding of material limitations for piezoelectric printing methods was gained. As a result, future work for the production of high-density sol-gel based microarrays is now conceivable through completed work that investigated bio-ink formulations amenable to piezoelectric printing methods.

Collectively, the work completed in microarray characterization and bio-ink formulation identified and highlighted instrument specific limitations. Building on this learned knowledge, future work towards the successful fabrication and characterization of piezoelectric printed sol-gel derived microarrays can be

achieved. In addition, future perspectives can also include microarray shelf stability, comparison between different proteins, expansion towards different biomolecules including cells and the use of other characterization techniques to gain more insight on the material-biological interface properties.

Chapter - Five | References

(1) Dahoumane, S. A.; Helka, B.-J.; Artus, M.; Aubie, B.; Brennan, J. D. In *Handbook of Nanomaterials Properties*; Bhushan, B., Luo, D., Schricker, S. R., Sigmund, W., Zauscher, S., Eds. 2014.

(2) Merrifield, R. B. *Journal of the American Chemical Society* **1963**, *85*, 2149.

(3) Furka, A. A.; Sebestyén, F. F.; Asgedom, M. M.; Dibó, G. G. *International Journal of Peptide and Protein Reseach* **1991**, *37*, 487.

(4) Houghten, R. A.; Pinilla, C.; Blondelle, S. E.; Appel, J. R.; Dooley, C. T.; Cuervo, J. H. *Nature* **1991**, *354*, 84.

(5) Lam, K. S.; Salmon, S. E.; Hersh, E. M.; Hruby, V. J.; Kazmierski, W. M.; Knapp, R. J. *Nature* **1991**, *354*, 82.

(6) Dibó, G. *Molecular Diversity* **2012**, *16*, 1.

(7) Lowe, G. *Chem. Soc. Rev.* **1995**, *24*, 309.

(8) Schena, M. M.; Shalon, D. D.; Davis, R. W.; Brown, P. O. *Science (New York, N.Y.)* **1995**, *270*, 467.

(9) Hook, A. L.; Anderson, D. G.; Langer, R.; Williams, P.; Davies, M. C.; Alexander, M. R. *Biomaterials* **2010**, *31*, 187.

(10) MacBeath, G.; Koehler, A. N.; Schreiber, S. L. *Journal of the American Chemical Society* **1999**, *121*, 7967.

(11) MacBeath, G.; Schreiber, S. L. *Science (New York, N.Y.)* **2000**, *289*, 1760.

(12) Zhu, H.; Bilgin, M.; Bangham, R.; Hall, D.; Casamayor, A.; Bertone, P.; Lan, N. N.; Jansen, R. R.; Bidlingmaier, S.; Houfek, T.; Mitchell, T. T.; Miller, P. P.; Dean, R. A.; Gerstein, M.; Snyder, M. M. *Science (New York, N.Y.)* **2001**, *293*, 2101.

(13) Ge, X.; Lebert, J. M.; Monton, M. R. N.; Lautens, L. L.; Brennan, J. D. *Chemistry of Materials* **2011**, *23*, 3685.

(14) Lee, S.; Kim, Y. S.; Jo, M.; Jin, M.; Lee, D.-k.; Kim, S. *Biochemical and Biophysical Research Communications* **2007**, *358*, 47.

(15) Monton, M. R. N.; Lebert, J. M.; Little, J. R. L.; Nair, J. J.; McNulty, J.; Brennan, J. D. *Analytical chemistry* **2010**, *82*, 9365.

(16) Barbulovic-Nad, I.; Lucente, M.; Sun, Y.; Zhang, M.; Wheeler, A. R.; Bussmann, M. *Critical Reviews in Biotechnology* **2006**, *26*, 237.

(17) Tsai, J.; Kim, C. J. In *Second Joint Embs-Bmes Conference 2002, Vols 1-3, Conference Proceedings* 2002, p 1632.

(18) Corporation, A. Online; Vol. 2013.

(19) Derby, B. *Annual Review of Materials Research* **2010**, *40*, 395.

(20) Tehan, E. C.; Higbee, D. J.; Wood, T. D.; Bright, F. V. *Analytical chemistry* **2007**, *79*, 5429.

(21) Anderson, D. G.; Levenberg, S.; Langer, R. *Nature biotechnology* **2004**, *22*, 863.

(22) Anderson, D. G.; Putnam, D.; Lavik, E. B.; Mahmood, T. A.; Langer, R. *Biomaterials* **2005**, *26*, 4892.

(23) Lynn, D. M.; Anderson, D. G.; Putnam, D.; Langer, R. *Journal of the American Chemical Society* **2001**, *123*, 8155.

(24) de Gans, B. J.; Duineveld, P. C.; Schubert, U. S. *Adv Mater* **2004**, *16*, 203.

(25) Kim, S.; Kim, Y.; Kim, P.; Ha, J.; Kim, K.; Sohn, M.; Yoo, J.-S.; Lee, J.; Kwon, J.-a.; Lee, K. N. *Analytical chemistry* **2006**, *78*, 7392.

(26) Zhang, R.; Liberski, A.; Khan, F.; Diaz-Mochon, J. J.; Bradley, M. *Chemical Communications* **2008**, 1317.

(27) de Gans, B.-J.; Schubert, U. S. *Langmuir* **2004**, *20*, 7789.

(28) Calvert, P. *Chemistry of Materials* **2001**, *13*, 3299.

(29) Jang, D.; Kim, D.; Moon, J. *Langmuir* **2009**, *25*, 2629.

(30) Taylor, M.; Urquhart, A. J.; Zelzer, M.; Davies, M. C.; Alexander, M. R. *Langmuir* **2007**, *23*, 6875.

(31) Gutmann, O.; Kuehlewein, R.; Reinbold, S.; Niekrawietz, R.; Steinert, C. P.; de Heij, B.; Zengerle, R.; Daub, M. *Lab on a Chip* **2005**, *5*, 675.

(32) Andrade, J. D.; Hlady, V.; Wei, A. P. *Pure and applied chemistry* **1992**, *64*, 1777.

(33) Karagulyan, H. K.; Gasparyan, V. K.; Decker, S. R. *Applied Biochemistry and Biotechnology* **2008**, *146*, 39.

(34) Weetall, H. H. *Applied Biochemistry and Biotechnology* **1993**, *41*, 157.

(35) Wilchek, M.; Bayer, E. A. *Analytical Biochemistry* **1988**, *171*, 1.

(36) Mallik, R.; Hage, D. S. *Journal of separation science* **2006**, *29*, 1686.

(37) Mallik, R.; Hage, D. S. *Journal of pharmaceutical and biomedical analysis* **2008**, *46*, 820.

(38) Ng, E. S. M.; Chan, N.; Lewis, D. F.; Hindsgaul, O.; Schriemer, D. C. *Nature Protocols* **2007**, *2*, 1907.

(39) Rupcich, N.; Nutiu, R.; Shen, Y.; Li, Y.; Brennan, J. D.; Springer: 2009, p 309.

(40) Muralidhar, R. V.; Jayachandran, G.; Singh, P. *CURRENT SCIENCE-BANGALORE-* **2001**, *81*, 263.

(41) Avnir, D.; Coradin, T.; Lev, O.; Livage, J. *Journal of Materials Chemistry* **2006**, *16*, 1013.

(42) Brennan, J. D. *Accounts of Chemical Research* **2007**, *40*, 827.

(43) Monton, M. R. N.; Forsberg, E. M.; Brennan, J. D. *Chemistry of Materials* **2011**, *24*, 796.

(44) Wu, X. J.; Choi, M. M. F. *Analytica Chimica Acta* **2004**, *514*, 219.

(45) Dickey, F. H. *The Journal of Physical Chemistry* **1955**, *59*, 695.

(46) Brinker, C. J.; Scherer, G. *Sol-Gel Science: The Physics and Chemistry of Sol-Gel Processing Academic Press*; New York, 1990; Vol. 19901.

(47) Avnir, D.; Kaufman, V. R. *Journal of non-crystalline solids* **1987**, *92*, 180.

(48) Ellerby, L. M.; Nishida, C. R.; Nishida, F.; Yamanaka, S. A.; Dunn, B.; Valentine, J. S.; Zink, J. I. *Science (New York, N.Y.)* **1992**, *255*, 1113.

(49) Brasack, I.; Böttcher, H.; Hempel, U. *Journal of sol-gel science and technology* **2000**, *19*, 479.

(50) Ferrer, M. L.; del Monte, F.; Levy, D. *Chemistry of Materials* **2002**, *14*, 3619.

(51) Bhatia, R. B.; Brinker, C. J.; Gupta, A. K.; Singh, A. K. *Chemistry of Materials* **2000**, *12*, 2434.

(52) Gill, I.; Ballesteros, A. *Journal of the American Chemical Society* **1998**, *120*, 8587.

(53) Brook, M. A.; Chen, Y.; Guo, K.; Zhang, Z.; Brennan, J. D. *Journal of Materials Chemistry* **2004**, *14*, 1469.

(54) Brook, M. A.; Chen, Y.; Guo, K.; Zhang, Z.; Jin, W.; Deisingh, A.; Cruz-Aguado, J. A.; Brennan, J. D. *Journal of sol-gel science and technology* **2004**, *31*, 343.

(55) Hodgson, R. J.; Besanger, T. R.; Brook, M. A.; Brennan, J. D. *Analytical chemistry* **2005**, *77*, 7512.

(56) Ishizuka, N.; Minakuchi, H.; Nakanishi, K.; Hirao, K.; Tanaka, N. *Colloids and Surfaces A: Physicochemical and Engineering Aspects* **2001**, *187-188*, 273.

(57) Hodgson, R. J.; Chen, Y.; Zhang, Z.; Tleugabulova, D.; Long, H.; Zhao, X.; Organ, M.; Brook, M. A.; Brennan, J. D. *Analytical chemistry* **2004**, *76*, 2780.

(58) Rupcich, N.; Goldstein, A.; Brennan, J. D. *Chemistry of Materials* **2003**, *15*, 1803.

(59) Rupcich, N.; Green, J. R. A.; Brennan, J. D. *Analytical chemistry* **2005**, *77*, 8013.

(60) Sakai-Kato, K. K.; Ishikura, K. *Analytical sciences : the international journal of the Japan Society for Analytical Chemistry* **2009**, *25*, 969.

(61) Besanger, T. R.; Easwaramoorthy, B.; Brennan, J. D. *Analytical chemistry* **2004**, *76*, 6470.

(62) Besanger, T. R.; Hodgson, R. J.; Guillon, D.; Brennan, J. D. *Analytica Chimica Acta* **2006**, *561*, 107.

(63) Fennouh, S.; Guyon, S.; Catherine, J.; Livage, J.; Roux, C. *Comptes Rendus de l'Académie des Sciences - Series IIC - Chemistry* **1999**, *2*, 625.

(64) Carrasquilla, C.; Lau, P. S.; Li, Y.; Brennan, J. D. *Journal of the American Chemical Society* **2012**, *134*, 10998.

(65) Carrasquilla, C.; Li, Y.; Brennan, J. D. *Analytical chemistry* **2011**, *83*, 957.

(66) Cho, E. J.; Bright, F. V. *Analytical chemistry* **2002**, *74*, 1462.

(67) Cho, E. J.; Tao, Z.; Tehan, E. C.; Bright, F. V. *Analytical chemistry* **2002**, *74*, 6177.

(68) Kim, Y. D.; Park, C. B.; Clark, D. S. *Biotechnology and Bioengineering* **2001**, *73*, 331.

(69) Park, C. B.; Clark, D. S. *Biotechnology and Bioengineering* **2002**, *78*, 229.

(70) Cho, E. J.; Tao, Z.; Tang, Y.; Tehan, E. C.; Bright, F. V.; Hicks, W. L.; Gardella, J. A.; Hard, R. *Applied spectroscopy* **2002**, *56*, 1385.

(71) Cho, E. J.; Bright, F. V. *Analytical chemistry* **2001**, *73*, 3289.

(72) Cho, E. J.; Bright, F. V. *Analytica Chimica Acta* **2002**, *470*, 101.

(73) Daivasagaya, D. S.; Yao, L.; Yung, K. Y.; Hajj-Hassan, M.; Cheung, M. C.; Chodavarapu, V. P.; Bright, F. V. *Sensors and Actuators B: Chemical* **2011**, *157*, 408.

(74) Tang, Y.; Tao, Z.; Bukowski, R. M.; Tehan, E. C.; Karri, S.; Titus, A. H.; Bright, F. V. *Analyst (Cambridge UK)* **2006**, *131*, 1129.

(75) Yao, L.; Yung, K. Y.; Chodavarapu, V. P.; Bright, F. V. *IEEE Transactions on Biomedical Circuits and Systems*, *5*, 189.

(76) Rupcich, N. *Analytica Chimica Acta* **2003**, *500*, 3.

(77) Doong, R.-a.; Lee, P.-S.; Anitha, K. *Biosensors and Bioelectronics* **2010**, *25*, 2464.

(78) Kwon, J.-a.; Lee, H.; Lee, K. N.; Chae, K.; Lee, S.; Lee, D.-k.; Kim, S. *Clinical chemistry* **2008**, *54*, 424.

(79) Park, S.-m.; Ahn, J.-Y.; Jo, M.; Lee, D.-k.; Lis, J. T.; Craighead, H. G.; Kim, S. *Lab on a Chip* **2009**, *9*, 1206.

(80) Ahn, J.-Y.; Lee, S. S.; Jo, M. M.; Kang, J. J.; Kim, E. E.; Jeong, O. C. O.; Laurell, T. T.; Kim, S. *Analytical chemistry* **2012**, *84*, 2647.

(81) FitzGerald, S. P. *Clinical chemistry* **2005**, *51*, 1165.

(82) Kingshott, P.; Andersson, G.; McArthur, S. L.; Griesser, H. J. *Current Opinion in Chemical Biology* **2011**, *15*, 667.

(83) Hook, A. L.; Chang, C.-Y.; Yang, J.; Luckett, J.; Cockayne, A.; Atkinson, S.; Mei, Y.; Bayston, R.; Irvine, D. J.; Langer, R.; Anderson, D. G.; Williams, P.; Davies, M. C.; Alexander, M. R. *Nature Biotechnology* **2012**.

(84) Celiz, A. D.; Hook, A. L.; Scurr, D. J.; Anderson, D. G.; Langer, R.; Davies, M. C.; Alexander, M. R. *Surface and Interface Analysis* **2012**, *45*, 202.

(85) Mei, Y.; Gerecht, S.; Taylor, M.; Urquhart, A.; Bogatyrev, S. R.; Cho, S. W.; Davies, M. C.; Alexander, M. R.; Langer, R. S.; Anderson, D. G. *Adv Mater* **2009**, *21*, 2781.

(86) Wang, H.; Chen, S.; Li, L.; Jiang, S. *Langmuir* **2005**, *21*, 2633.

(87) BonafÉ, N.; Chaussepied, P.; Capony, J. P.; Derancourt, J.; Kassab, R. *European Journal of Biochemistry* **1993**, *213*, 1243.